Asymptotically exact strain-gradient models for nonlinear slender elastic structures: a systematic derivation method

Claire Lestringant[a], Basile Audoly[b]

[a]*Mechanics & Materials, Department of Mechanical and Process Engineering, ETH Zürich, 8092 Zürich, Switzerland*
[b]*Laboratoire de mécanique des solides, CNRS, Institut Polytechnique de Paris, Palaiseau, France*

Abstract

We propose a general method for deriving one-dimensional models for nonlinear structures. It captures the contribution to the strain energy arising not only from the macroscopic elastic strain as in classical structural models, but also from the strain gradient. As an illustration, we derive one-dimensional strain-gradient models for a hyper-elastic cylinder that necks, an axisymmetric membrane that produces bulges, and a two-dimensional block of elastic material subject to bending and stretching. The method offers three key advantages. First, it is nonlinear and accounts for large deformations of the cross-section, which makes it well suited for the analysis of localization in slender structures. Second, it does not require any *a priori* assumption on the form of the elastic solution in the cross-section, i.e., it is Ansatz-free. Thirdly, it produces one-dimensional models that are asymptotically exact when the macroscopic strain varies on a much larger length scale than the cross-section diameter.

Keywords: A. Localization B. elastic material, B. finite strain, C. asymptotic analysis, C. energy methods

1. Introduction

There exists a variety of models for slender structures, going much beyond the traditional models for the stretching of bars and the bending of beams. The applicability of classical models being limited to materials having linear, homogeneous and isotropic elastic properties, a number of extensions have been considered to account for different elastic behaviors such as hyperelastic materials (Cimetière et al., 1988) or more specifically nematic elastomers (Agostiniani et al., 2016), for inhomogeneous elastic properties in the cross-section, for the presence of natural curvature or twist (Freddi et al., 2016) or more generally for the existence of inhomogeneous pre-stress in the cross-section (Lestringant and Audoly, 2017). As the classical rod models are inapplicable if the cross-section itself is a slender 2d domain, specific models have been derived, e.g., to address inextensible ribbons (Sadowsky, 1930; Wunderlich, 1962), as well as thin walled beams having a flat (Freddi et al., 2004) or curved (Hamdouni and Millet, 2006) cross-section. The classical models are inapplicable as well in the presence of a large contrast of elastic moduli within the cross-sections, as happens for sandwiched beams: in this case, the presence of shear is often accounted for using the Timoshenko beam model. Specific models are also required to account for physical effects such as the interaction with a magnetic field (Geymonat et al., 2018) or surface tension arising in soft beams immersed in a fluid (Xuan and Biggins, 2017).

One can easily get lost in view of not only the multiplicity of these models but also their justification (or lack thereof). Rigorous justifications based on asymptotic expansions have made use of restrictive assumptions: the work in this direction was initiated in the context of linear elasticity (Bermudez and Viaño, 1984; Sanchez-Hubert and Sanchez Palencia, 1999), and extended to finite elasticity under specific assumptions regarding material symmetries (Cimetière et al., 1988). The different models, such as Navier-Bernoulli beams, Timoshenko beams, Vlasov beams, inextensible ribbons, etc., are justified by different arguments each, and a unified justification method is lacking. There are many phenomena in slender

structures for which no asymptotically justified 1d model is available, such as the ovalization of tubes subjected to bending (Calladine, 1983) or pinching (Mahadevan et al., 2007) and the propagative instabilities in shallow panels (Kyriakides and Chang, 1991).

In some work, one-dimensional (1d) models have been proposed based on kinematic hypotheses. This is the case, for instance, for the analysis localization in hyperelastic cylinders (Coleman and Newman, 1988) and tape springs (Picault et al., 2016). Even when these kinematic hypotheses turn out to be valid, their domain of validity is typically limited and dependent, in a hidden way, on the simplifying assumptions of the model. For instance, the most common assumptions used to derive the classical theory of beams is that cross-sections remain planar and perpendicular to the center line, and that the shear in the plane of the cross-sections is zero. These assumptions are incorrect unless specific material symmetries are applicable, which is ill-appreciated. Moreover, they cannot be used to derive higher-order models, as discussed by Audoly and Hutchinson (2016).

This paper proposes a systematic and rigorous dimension reduction method for obtaining 1d models for nonlinear slender elastic structures, which works under broad assumptions. The main features of the method are as follows. The reduction method can start from a variety of models, such as a hyperelastic model for cylinder (e.g., for the stretching of bars), a nonlinear model for a thin membrane (e.g., for the analysis of bulges in axisymmetric balloons) or a shell model (e.g., for the tape spring problem). It can handle arbitrary elastic constitutive laws (including nonlinear and anisotropic ones), arbitrary pre-stress distributions in the cross-section, and inhomogeneous material properties in the cross-section. The mechanical and geometrical properties of the structure are assumed to be invariant in the longitudinal direction; the extension to slowly variable properties is straightforward, as discussed in §6. Nonlinearity of both the elastic and geometric types are permitted, and large spatial variations in the deformed shape of the cross-sections are accounted for. No *a priori* kinematic hypothesis is made, the microscopic displacement being found by solving the equations of elasticity. Our reduction method is built on a two-scale expansion, assuming slow variations in the longitudinal directions. As such, it is asymptotically exact. Its justification is based on a formal expansion, not on a rigorous proof. We hope that our formal argument can be turned into a rigorous one in the future.

An important asset of the method is that it captures the gradient effect, i.e., the dependence of the strain energy on the gradient of strain and not just on the strain. This makes it possible to derive higher-order reduced models offering the following advantages: (*i*) they feature faster convergence towards the solution of the full (non-reduced) problem and (*ii*) they are well-suited to the analysis of localization in slender structures. Localization is ubiquitous in slender structures, from neck formation in polymer bars under traction (G'Sell et al., 1983), to beading in cylinders made up of soft gels (Matsuo and Tanaka, 1992; Mora et al., 2010), to bulges produced by the inflation of cylindrical party balloons (Kyriakides and Chang, 1990), and to kinks in bent tape springs (Seffen and Pellegrino, 1999). Classical reduced models depending on strain only cannot resolve the sharp interfaces that result from localization, and are mathematically ill-posed. By contrast, higher-order models capturing the dependence on the gradient of strain allows the interfaces to be resolved and are well-posed in the context of localization. In prior work, asymptotic 1d strain-gradient models have been obtained as refinements over the standard theory for linearly elastic beams (Trabucho and Viaño, 1996; Buannic and Cartaud, 2000), inextensible ribbons (Sadowsky, 1930; Wunderlich, 1962) and thin-walled beams (Freddi et al., 2004). The possibility of using 1d models to analyze localization in slender structures easily and accurately has emerged recently in the context of necking in bars and bulging in balloons (Audoly and Hutchinson, 2016; Lestringant and Audoly, 2018). Several other localization phenomena could be better understood if 1d models were available.

Our method can be described in general terms as follows. First, we introduce the so-called canonical form, which is a unified and abstract formulation into which the various structural models for slender structures can be cast. The canonical form serves as a starting point for the reduction process. The set of degrees of freedom are split between (master) macroscopic degrees of freedom which are retained in the 1d model, and (slave) microscopic degrees of freedom which are relaxed; the choice of which degrees of freedom are retained as master is left to the user. Next, the asymptotic expansion is carried out: the equations of elasticity are expanded about a configuration having finite and inhomogeneous pre-strain, whereby each cross-section is in a state parameterized by the local value of the macroscopic degrees of freedom. This

expansion is implemented as a series of steps (i.e., a mere recipe, albeit a slightly technical one at places) which ultimately yields a 1d elastic potential governing the reduced model. Classical structural model, such as the Euler-Bernoulli beam model, are recovered at the dominant order while corrections depending on the strain gradient are obtained at the subdominant order. In this first paper, the general method is presented and illustrated on simple examples for which the 1d strain-gradient model is already known from the literature; the method will be applied to original problems in future work.

In section 2, we give a general account of the reduction method: the series of steps needed to carry out the reduction are listed. In Sections 3 to 5, three examples of applications are worked out, by order of increasing complexity: we establish the 1d models for the bulging of inflated membranes, for a linearly elastic block in 2d, and for an axisymmetric hyperelastic cylinder. In Section 6, we conclude and make a few general remarks about the method. Appendix A presents a detailed proof of the reduction method. Appendix B provides the detailed calculations for the analysis of an axisymmetric cylinder.

In mathematical formula, we use bold face symbols for vectors and tensors. Their components are denoted using plain typeface with a subscript, as in $\boldsymbol{h} = (h_1, h_2)$. Functions of a cross-sectional coordinate are denoted by surrounding their generic values using curly braces, with their dummy argument in subscript, as in $f = \{f(T)\}_T$. We denote by S the longitudinal coordinate. In our notation, the primes will be reserved for the derivation with respect to the longitudinal coordinate S,

$$f' = \frac{\mathrm{d}f}{\mathrm{d}S}.$$

2. Main results

We present the dimension reduction method in a generic and abstract form that will be applied to specific structures in the forthcoming sections. We limit attention to a practical description of the method: the method is justified in full details separately in Appendix A.

2.1. Starting point: full model in canonical form

The elastic model used as a starting point for the dimension reduction will be referred to as the *full model*. One can use a variety of full models, such as an axisymmetric membrane model (for the analysis of bulges in balloons), a hyperelastic cylinder (for the analysis of necking) or a shell model (for the analysis of a tape spring). We start by casting the full models into a standardized form, called the *canonical form*, which exposes their common properties and hides their specificities. The conversion of particular structural models into the canonical form is not discussed here, and will be demonstrated based on examples in the following sections.

We assume that the structure is invariant along its longitudinal direction in the reference configuration, i.e., it is a block in two dimensions or a prismatic solid in three dimensions. The reference configuration does not need to be stress-free: naturally curved or twisted elastic rods for instance can be handled. The extension to structures whose geometric or mechanical properties are not invariant but slowly varying in the longitudinal direction is straightforward and will be discussed at the end of the paper. We denote by S a Lagrangian coordinate along the long dimension of the structure. The range of variation of S is denoted as $0 \leq S \leq L$, where L typically denotes the natural length of the structure. The parameter S is used to label the cross-sections, see figure 1(a).

Let $\boldsymbol{E}(S)$ be the strain map over a particular cross-section S in the current configuration, as sketched in figure 1(b). By strain *map*, we mean that $\boldsymbol{E}(S)$ is the restriction to a particular cross-section of the set of strain measures relevant to the particular structural model. If we are dealing with a hyperelastic cylinder, for instance, $\boldsymbol{E}(S)$ collects all the strain components $\{E_{SS}(\cdot,\cdot), E_{SX}(\cdot,\cdot), E_{XX}(\cdot,\cdot), E_{SY}(\cdot,\cdot), E_{YY}(\cdot,\cdot), E_{XY}(\cdot,\cdot)\}$, each taking the cross-section coordinates (X, Y) as arguments.

Next, we introduce two mathematical objects in each cross-section: a vector of *macroscopic* strain $\boldsymbol{h}(S) = (h_1(S), h_2(S), \ldots)$ made up of the strain measures that will survive in the 1d model, and a set of *microscopic* degrees of freedom $\boldsymbol{y}(S)$ that will be ultimately be eliminated. Their exact definitions vary, but typically $\boldsymbol{h}(S)$ is the (apparent) 1d strain, as calculated from the center line passing through the centers

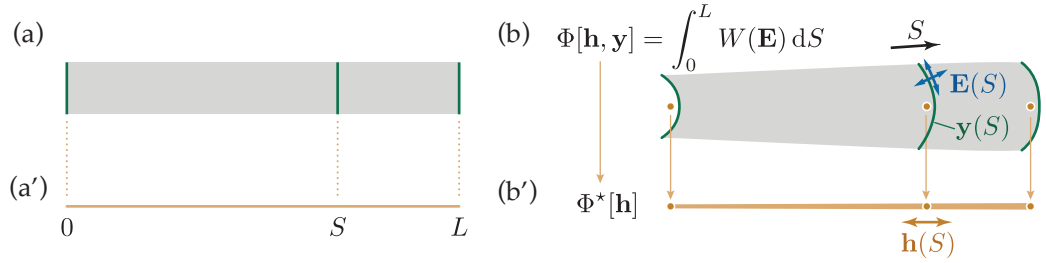

Figure 1: Dimension reduction for an abstract slender structure. *Left column* (a,a'): reference configuration highlighting a particular cross-section with coordinate S. *Right-hand side column* (b,b'): deformed configuration. *Top row* (a,b): full model used as a staring point, including a microscopic displacement $\boldsymbol{y}(S)$ and a microscopic strain $\boldsymbol{E}(S)$. *Bottom row* (a',b'): equivalent 1d model obtained by dimension reduction, in which the details at the scale of cross-section are effectively hidden.

of all the cross-section, while $\boldsymbol{y}(S)$ parameterizes the deformation of the cross-section relative to the center line. Typically, $\boldsymbol{h}(S)$ is a vector of low dimension, while $\boldsymbol{y}(S)$ is a (collection of) functions defined over the cross-sections, i.e., an infinite-dimensional vector. For the axisymmetric hyperelastic cylinder, for instance, $\boldsymbol{h}$ is made up of a single entry, the axial stretch, while $\boldsymbol{y}(S)$ is the cross-sectional map of displacement.

Together, the macroscopic strain $\boldsymbol{h}(S)$ and microscopic degrees of freedom $\boldsymbol{y}(S)$ determine the current configuration of the structure (up to a rigid-body motion) hence the microscopic strain $\boldsymbol{E}$. Therefore, each particular structural model prescribes a method for calculating the cross-sectional strain map $\boldsymbol{E}(S)$ in terms of $\boldsymbol{h}$, $\boldsymbol{y}$ and their longitudinal derivatives,

$$\boldsymbol{E}(S) = \boldsymbol{E}(\boldsymbol{h}(S), \boldsymbol{h}'(S); \boldsymbol{y}(S), \boldsymbol{y}'(S), \boldsymbol{y}''(S)). \tag{2.1}$$

In the example of the cylinder, the longitudinal strain E_{SS} depends on the longitudinal gradient of the displacement, hence the dependence of $\boldsymbol{E}$ on $\boldsymbol{y}'$.

Since $\boldsymbol{y}(S)$ is a function defined on the cross-sections, the function $\boldsymbol{E}$ in the right-hand side of (2.1) is a *functional* when the domain of the cross-section is continuous. Since $\boldsymbol{E}(S)$ is a *map* of strain over the cross-section, any dependence of the strain on the transverse gradients of displacement is hidden in the definition of $\boldsymbol{E}$ above. By contrast, we make sure that the dependence on longitudinal gradients takes place explicitly through the supplied argument $\boldsymbol{y}'$ (and possibly $\boldsymbol{y}''$). The additional dependence on $\boldsymbol{y}''$ will allow us to handle the bending of plates or shells without change. It is easy to take into account an additional dependence of $\boldsymbol{E}$ on higher-order gradients of $\boldsymbol{h}(S)$ or $\boldsymbol{y}(S)$; this does not affect any of the results.

In terms of the strain map $\boldsymbol{E}(S)$, the structural model defines a density of strain energy $W(\boldsymbol{E})$ per unit length $\mathrm{d}S$. The strain energy of the structure therefore writes

$$\Phi[\boldsymbol{h}, \boldsymbol{y}] = \int_0^L W(\boldsymbol{E}(\boldsymbol{h}(S), \boldsymbol{h}'(S); \boldsymbol{y}(S), \boldsymbol{y}'(S), \boldsymbol{y}''(S)))\,\mathrm{d}S, \tag{2.2}$$

where the square brackets emphasize the functional dependence on the arguments.

Some structural models are conveniently expressed by imposing kinematic constraints $\boldsymbol{q}(\boldsymbol{y}) = \boldsymbol{0}$ on the microscopic displacement, where $\boldsymbol{q}(\boldsymbol{y}) = (q_1(\boldsymbol{y}), q_2(\boldsymbol{y}), \ldots)$. For structures whose cross-section involve infinitely many degrees of freedom, $\boldsymbol{y}(S)$ is (a set of) functions defined in the cross-sections, i.e., $\boldsymbol{q}$ is a functional. We focus attention on kinematic constraints that are linear and independent of S. These assumptions can be relaxed easily. For structures that are free of kinematic constraints, we set $\boldsymbol{q}$ as the empty vector, $\boldsymbol{q}(\boldsymbol{y}) = ()$, implying that any term such as $\boldsymbol{q}(\boldsymbol{y}) \cdot \boldsymbol{x} = 0$ must be discarded in the following.

We deal with dimension reduction by addressing the following relaxation problem: the macroscopic strain $\boldsymbol{h}(S)$ is prescribed and we seek the microscopic variables $\boldsymbol{y}(S)$ making the strain energy $\Phi[\boldsymbol{h}, \boldsymbol{y}]$ stationary, subject to the kinematic constraint

$$\forall S \quad \boldsymbol{q}(\boldsymbol{y}(S)) = 0. \tag{2.3}$$

Our goal is to calculate the relaxed strain energy $\Phi^\star$ in terms of the macroscopic strain $\boldsymbol{h}(S)$. It can be

obtained by inserting the optimal microscopic displacement $\boldsymbol{y}(S)$ into Φ, as in

$$\Phi^\star[\boldsymbol{h}] = \min_{\boldsymbol{y}:(\forall S)\boldsymbol{q}(\boldsymbol{y}(S))=0} \Phi[\boldsymbol{h},\boldsymbol{y}]. \tag{2.4}$$

This paper derives an expansion of $\Phi^\star[\boldsymbol{h}]$ in successive derivatives of $\boldsymbol{h}(S)$ using an asymptotic method. Note that the relaxed energy $\Phi^\star[\boldsymbol{h}]$ is 1d: it no longer makes any reference to the cross-sectional degrees of freedom. Once $\Phi^\star[\boldsymbol{h}]$ has been obtained, the equilibrium equations for the 1d model can be derived using standard variational techniques.

2.2. Analysis of homogeneous solutions

The first step in our analysis is to characterize homogeneous solutions under finite strain. To do so, we focus attention on the case where both the macroscopic strain $\boldsymbol{h} = (h_1, h_2, \ldots)$ and the microscopic displacement $\boldsymbol{y}$ are independent [1] of S. The strain for homogeneous solutions $\tilde{\boldsymbol{E}}(\boldsymbol{h},\boldsymbol{y})$ is obtained by setting $\boldsymbol{h}' = \boldsymbol{0}$, $\boldsymbol{y}' = \boldsymbol{0}$ and $\boldsymbol{y}'' = \boldsymbol{0}$ in (2.1) as

$$\tilde{\boldsymbol{E}}(\boldsymbol{h},\boldsymbol{y}) = \boldsymbol{E}(\boldsymbol{h},\boldsymbol{0};\boldsymbol{y},\boldsymbol{0},\boldsymbol{0}). \tag{2.5}$$

For a given value of the macroscopic strain $\boldsymbol{h} = (h_1, h_2, \ldots)$, we seek the microscopic displacement $\boldsymbol{y} = \boldsymbol{y}_{\boldsymbol{h}} = \boldsymbol{y}_{(h_1,h_2,\ldots)}$ such that the cross-sections are in equilibrium. To do so, we seek the value(s) of $\boldsymbol{y}$ that make stationary the strain energy per unit length $W(\tilde{\boldsymbol{E}}(\boldsymbol{h},\boldsymbol{y}))$, among those satisfying the kinematic constraint $\boldsymbol{q}(\boldsymbol{y})$. This yields the variational problem

$$\left\{\begin{array}{ll} \forall \hat{\boldsymbol{y}} & -\frac{\mathrm{d}W}{\mathrm{d}\boldsymbol{E}}(\tilde{\boldsymbol{E}}(\boldsymbol{h},\boldsymbol{y}_{\boldsymbol{h}}))\cdot\left(\frac{\partial\tilde{\boldsymbol{E}}}{\partial\boldsymbol{y}}(\boldsymbol{h},\boldsymbol{y}_{\boldsymbol{h}})\cdot\hat{\boldsymbol{y}}\right)+\boldsymbol{f}_{\boldsymbol{h}}\cdot\boldsymbol{q}(\hat{\boldsymbol{y}})=0 \\ \boldsymbol{q}(\boldsymbol{y}_{\boldsymbol{h}})=\boldsymbol{0}, & \end{array}\right. \tag{2.6}$$

where the unknown $\boldsymbol{f}_{\boldsymbol{h}}$ is a Lagrange multiplier enforcing the constraint on the second line ($\boldsymbol{f}_h$ can be interpreted as the macroscopic load that is required for the homogeneous solution to be globally in equilibrium, such as a transverse external load in the case of a rod subject to a combination of uniform tension and bending). For structures whose cross-sections define a continuous domain in the plane, $W(\boldsymbol{E})$ is a functional taking on scalar values, and $\frac{\mathrm{d}W}{\mathrm{d}\boldsymbol{E}}(\boldsymbol{E})\cdot\delta\boldsymbol{E}$ denotes the Gâteaux derivative at $\boldsymbol{E}$ in the direction $\delta\boldsymbol{E}$. For structures possessing discrete cross-sectional degrees of freedom, $\frac{\mathrm{d}W}{\mathrm{d}\boldsymbol{E}}(\boldsymbol{E})$ the gradient of the function $W(\boldsymbol{E})$.

Equation (2.6) warrants stationarity with respect to the microscopic displacement, but not with respect to the macroscopic strain. For a solution of these equations to represent an actual equilibrium, one would need to set up macroscopic forces conjugate to the macroscopic strain, labeled $\boldsymbol{F}_{\boldsymbol{h}}$ in figure 2. If the structure is an elastic cylinder, for instance, equation (2.6) imposes the contraction of cross-sections by Poisson's effect; to maintain the global equilibrium, a macroscopic tensile load, not discussed here, would be required. Macroscopic load do not enter into the dimension reduction process: they can be introduced directly in the 1d model, after the dimension reduction.

Equation (2.6) is a non-linear elasticity problem defined on the cross-section: the longitudinal variable has been removed. This problem can be solved, most often analytically (see the examples in the following sections) or in some cases numerically. By solving equation (2.6) for $\boldsymbol{y}_{\boldsymbol{h}}$ and $\boldsymbol{f}_{\boldsymbol{h}}$ for any value of the macroscopic strain $\boldsymbol{h}$, one obtains a *catalog* of homogeneous solutions, which is at the heart of the dimension reduction method. It is derived without any approximation: the catalog is made up of *nonlinear* solutions.

In terms of the catalog of microscopic displacement $\boldsymbol{y}_{\boldsymbol{h}}$, we can define the homogeneous strain $\boldsymbol{E}_{\boldsymbol{h}}$, the homogeneous strain energy density $W_{\mathrm{hom}}(\boldsymbol{h})$, the homogeneous pre-stress $\boldsymbol{\Sigma}_{\boldsymbol{h}}$, and the homogeneous tangent stiffness, as follows,

$$\begin{array}{rcl} \boldsymbol{E}_{\boldsymbol{h}} & = & \tilde{\boldsymbol{E}}(\boldsymbol{h},\boldsymbol{y}_{\boldsymbol{h}}) \\ W_{\mathrm{hom}}(\boldsymbol{h}) & = & W(\boldsymbol{E}_{\boldsymbol{h}}) \\ \boldsymbol{\Sigma}_{\boldsymbol{h}} & = & \frac{\mathrm{d}W}{\mathrm{d}\boldsymbol{E}}(\boldsymbol{E}_{\boldsymbol{h}}) \\ \boldsymbol{K}_{\boldsymbol{h}} & = & \frac{\mathrm{d}^2W}{\mathrm{d}\boldsymbol{E}^2}(\boldsymbol{E}_{\boldsymbol{h}}). \end{array} \tag{2.7}$$

[1] Here, we are assuming that the splitting of the microscopic strain $\boldsymbol{E}(S)$ into master ($\boldsymbol{h}(S)$) and slave ($\boldsymbol{y}(S)$) degrees of freedom has been set up in such a way that homogeneous solutions correspond to constant $\boldsymbol{h}$ and constant $\boldsymbol{y}$. Any reasonable choice of $\boldsymbol{h}(S)$ and $\boldsymbol{y}(S)$ satisfies this property.

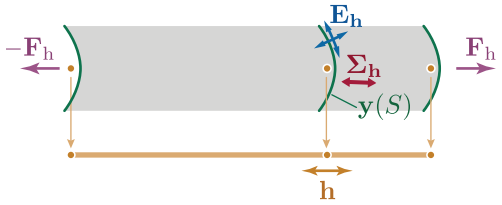

Figure 2: A homogeneous solution with uniform macroscopic strain $\boldsymbol{h}$: microscopic displacement $\boldsymbol{y}_{\boldsymbol{h}}$, microscopic strain $\boldsymbol{E}_{\boldsymbol{h}}$ and microscopic stress $\boldsymbol{\Sigma}_{\boldsymbol{h}}$. Note that the we are not interested at this stage in calculating the external loading $\boldsymbol{F}_{\boldsymbol{h}}$ that maintains equilibrium with respect to the macroscopic variables.

In our notation, the homogeneous quantities are either subscripted with the letters 'hom', as in W_{hom}, or simply by the vector of macroscopic strain $\boldsymbol{h} = (h_1, h_2, \dots)$ on which they depend.

2.3. Reduced models without gradient effect

Most 1d models used for slender structures depend on macroscopic strain variables, but not on their gradients. The Euler-Bernoulli rod model, for instance, depends on curvature and twist and not on their gradients. These standard structural models are governed by the strain energy

$$\Phi^\star[\boldsymbol{h}] \approx \int_0^L W_{\text{hom}}(\boldsymbol{h}(S))\,\mathrm{d}S \qquad \text{(reduction without strain gradient)},$$

and can therefore be derived directly from the catalog of homogeneous solutions. If we start from an elastic block, for example, and choose the axial strain and curvature as macroscopic variables, the strain energy $\int_0^L W_{\text{hom}}(\boldsymbol{h}(S))\,\mathrm{d}S$ defines a classical beam model (see §4.7). Note that the 1d model associated with the energy functional $\Phi^\star[\boldsymbol{h}]$ above might suffer from poorer convexity properties than the original 3d model; this happens typically when a string model is derived (*i.e.*, when $\boldsymbol{h}(S)$ is set up to include just an axial strain variable, so that there is no bending energy in the resulting 1d model), and in this case an additional relaxation step is needed to remove the unphysical part of the constitutive law predicting axial compression (Acerbi et al., 1991).

So far, our method carries out dimension reduction without strain gradient. It does so without using any kinematic assumption and works under very general conditions: no material symmetry has been assumed, and it can handle inhomogeneous cross-sections and nonlinear elastic materials.

2.4. Microscopic correction, energy expansion

We return to the main focus of our work, which is on capturing *strain-gradient* effects. Given a distribution of macroscopic strain $\boldsymbol{h}(S)$ with $0 \le S \le L$, we aim at calculating the optimal microscopic displacement $\boldsymbol{y}(S)$ and, thus, the relaxed energy $\Phi^\star$ appearing in equation (2.4). We do so by assuming slow variations in the longitudinal direction: a proper stretched variable is introduced in the detailed proof of Appendix A, but it will suffice here to assume that the successive longitudinal derivatives of quantities such as $\boldsymbol{h}(S)$ scale like $\boldsymbol{h} = \mathcal{O}(1)$, $\boldsymbol{h}' = \mathcal{O}(\gamma)$, $\boldsymbol{h}'' = \mathcal{O}(\gamma^2)$, etc., where $\gamma \ll 1$ is a slenderness parameter.

We seek the microscopic displacement $\boldsymbol{y}(S)$ that achieves the optimum in equation (2.4) in the form:

$$\boldsymbol{y}(S) = \boldsymbol{y}_{\boldsymbol{h}(S)} + \boldsymbol{z}(S). \tag{2.8}$$

In words, we use the leading order microscopic displacement $\boldsymbol{y}_{\boldsymbol{h}(S)}$ obtained by looking up our catalog of homogeneous solutions $\boldsymbol{h} \mapsto \boldsymbol{y}_{\boldsymbol{h}}$ as a first approximation; this look-up is performed with the parameter $\boldsymbol{h}$ set to the local prescribed value of the macroscopic strain, $\boldsymbol{h} = \boldsymbol{h}(S)$. We refine this approximation by a correction $\boldsymbol{z}(S)$ proportional to the gradient term $\boldsymbol{h}'$, which we calculate next.

To reflect the change of unknown from $\boldsymbol{y}(S)$ to $\boldsymbol{z}(S)$ in (2.8), let us first define the function $\boldsymbol{e}_{\boldsymbol{h}}$ that yields the strain as in (2.1):

$$\boldsymbol{e}_{\boldsymbol{h}}(\boldsymbol{h}^\dagger, \boldsymbol{h}^\ddagger; \boldsymbol{z}, \boldsymbol{z}^\dagger, \boldsymbol{z}^\ddagger) = \boldsymbol{E}(\boldsymbol{h}, \boldsymbol{h}^\dagger; \boldsymbol{y}_{\boldsymbol{h}} + \boldsymbol{z}, \boldsymbol{h}^\dagger \cdot \nabla \boldsymbol{y}_{\boldsymbol{h}} + \boldsymbol{z}^\dagger, \boldsymbol{h}^\ddagger \cdot \nabla \boldsymbol{y}_{\boldsymbol{h}} + \boldsymbol{h}^\dagger \cdot \nabla^2 \boldsymbol{y}_{\boldsymbol{h}} \cdot \boldsymbol{h}^\dagger + \boldsymbol{z}^\ddagger). \tag{2.9}$$

The variables bearing a dag (†) or a double dag (‡) are those that will be set later to the local value of the first or second gradients. The quantity $\boldsymbol{h}^\dagger$, for instance, is a dummy variable that will be set later to $\boldsymbol{h}^\dagger = \boldsymbol{h}'(S)$. Besides, the ∇ in equation (2.9) stands for gradients with respect to the macroscopic strain $\boldsymbol{h}$,

$$\nabla^k \boldsymbol{y}_{\boldsymbol{h}} = \frac{\mathrm{d}^k \boldsymbol{y}_{\boldsymbol{h}}}{\mathrm{d}\boldsymbol{h}^k}. \tag{2.10}$$

Anticipating on the fact that we will need to expand the strain in (2.9), we define the *structure coefficients* $\boldsymbol{e}^{ij}_{klm}(\boldsymbol{h})$ as the gradients of $\boldsymbol{e}_{\boldsymbol{h}}$, evaluated at a homogeneous solution: for any set of integers (i, j, k, l, m),

$$\boldsymbol{e}^{ij}_{klm}(\boldsymbol{h}) = \frac{\partial^{(i+j+k+l+m)} \boldsymbol{e}_{\boldsymbol{h}}}{[\partial \boldsymbol{h}^\dagger]^i \, [\partial \boldsymbol{h}^\ddagger]^j \, [\partial \boldsymbol{z}]^k \, [\partial \boldsymbol{z}^\dagger]^l \, [\partial \boldsymbol{z}^\ddagger]^m} (\boldsymbol{0}, \boldsymbol{0}; \boldsymbol{0}, \boldsymbol{0}, \boldsymbol{0}). \tag{2.11}$$

Note that the upper set of indices correspond to gradients with respect to the gradients of the macroscopic strain parameters $\boldsymbol{h}^\dagger$ and $\boldsymbol{h}^\ddagger$ while the lower set of indices correspond to gradients with respect to the microscopic variable $\boldsymbol{z}$ and its gradients $\boldsymbol{z}^\dagger$ and $\boldsymbol{z}^\ddagger$. The quantities $\boldsymbol{e}^{ij}_{klm}(\boldsymbol{h})$ are either tensors, or operators (if the cross-sectional degrees of freedom are continuous and at least one integer among k, l, m are non-zero): they will always appear contracted i times with $\boldsymbol{h}^\dagger$, j times with $\boldsymbol{h}^\ddagger$, k times with $\boldsymbol{z}$, etc. Each one of these contractions will be denoted by a dot, representing either the standard contraction of tensors or the application of the operator.

The Taylor expansion of the strain (2.9) near a homogeneous solution can be written in terms of the structure coefficients as

$$\boldsymbol{e}_{\boldsymbol{h}}(\boldsymbol{h}^\dagger, \boldsymbol{h}^\ddagger; \boldsymbol{z}, \boldsymbol{z}^\dagger, \boldsymbol{z}^\ddagger) = \boldsymbol{e}_{\boldsymbol{h}}(\boldsymbol{0}, \boldsymbol{0}; \boldsymbol{0}, \boldsymbol{0}, \boldsymbol{0}) + \boldsymbol{e}^{10}_{000}(\boldsymbol{h}) \cdot \boldsymbol{h}^\dagger + \boldsymbol{e}^{00}_{100}(\boldsymbol{h}) \cdot \boldsymbol{z} + \frac{1}{2} \left(2\, \boldsymbol{h}^\dagger \cdot \boldsymbol{e}^{10}_{100}(\boldsymbol{h}) \cdot \boldsymbol{z} + \cdots \right) + \cdots$$

Structure coefficients will be calculated explicitly in the second part of the paper, when explicit structures are considered.

In terms of the structure coefficients, we further introduce the following operators,

$$\begin{aligned}
\boldsymbol{A}_{\boldsymbol{h}} \cdot \boldsymbol{h}^\dagger &= \boldsymbol{\Sigma}_{\boldsymbol{h}} \cdot (\boldsymbol{e}^{10}_{000}(\boldsymbol{h}) \cdot \boldsymbol{h}^\dagger) \\
\boldsymbol{C}^{(0)}_{\boldsymbol{h}} \cdot \boldsymbol{h}^\ddagger &= \boldsymbol{\Sigma}_{\boldsymbol{h}} \cdot (\boldsymbol{e}^{01}_{000}(\boldsymbol{h}) \cdot \boldsymbol{h}^\ddagger) \\
\boldsymbol{C}^{(1)}_{\boldsymbol{h}} \cdot \boldsymbol{z}^\dagger &= \boldsymbol{\Sigma}_{\boldsymbol{h}} \cdot (\boldsymbol{e}^{00}_{010}(\boldsymbol{h}) \cdot \boldsymbol{z}^\dagger) \\
\tfrac{1}{2}\, \boldsymbol{h}^\dagger \cdot \boldsymbol{B}^{(0)}_{\boldsymbol{h}} \cdot \boldsymbol{h}^\dagger &= \tfrac{1}{2} (\boldsymbol{e}^{10}_{000}(\boldsymbol{h}) \cdot \boldsymbol{h}^\dagger) \cdot \boldsymbol{K}_{\boldsymbol{h}} \cdot (\boldsymbol{e}^{10}_{000}(\boldsymbol{h}) \cdot \boldsymbol{h}^\dagger) + \tfrac{1}{2}\, \boldsymbol{\Sigma}_{\boldsymbol{h}} \cdot (\boldsymbol{h}^\dagger \cdot \boldsymbol{e}^{20}_{000}(\boldsymbol{h}) \cdot \boldsymbol{h}^\dagger) - \boldsymbol{h}^\dagger \cdot \nabla \boldsymbol{C}^{(0)}_{\boldsymbol{h}} \cdot \boldsymbol{h}^\dagger \\
\boldsymbol{h}^\dagger \cdot \boldsymbol{B}^{(1)}_{\boldsymbol{h}} \cdot \boldsymbol{z} &= (\boldsymbol{e}^{10}_{000}(\boldsymbol{h}) \cdot \boldsymbol{h}^\dagger) \cdot \boldsymbol{K}_{\boldsymbol{h}} \cdot (\boldsymbol{e}^{00}_{100}(\boldsymbol{h}) \cdot \boldsymbol{z}) + \boldsymbol{\Sigma}_{\boldsymbol{h}} \cdot (\boldsymbol{h}^\dagger \cdot \boldsymbol{e}^{10}_{100}(\boldsymbol{h}) \cdot \boldsymbol{z}) - \boldsymbol{h}^\dagger \cdot \nabla \boldsymbol{C}^{(1)}_{\boldsymbol{h}} \cdot \boldsymbol{z} \\
\tfrac{1}{2}\, \boldsymbol{z} \cdot \boldsymbol{B}^{(2)}_{\boldsymbol{h}} \cdot \boldsymbol{z} &= \tfrac{1}{2} (\boldsymbol{e}^{00}_{100}(\boldsymbol{h}) \cdot \boldsymbol{z}) \cdot \boldsymbol{K}_{\boldsymbol{h}} \cdot (\boldsymbol{e}^{00}_{100}(\boldsymbol{h}) \cdot \boldsymbol{z}) + \tfrac{1}{2}\, \boldsymbol{\Sigma}_{\boldsymbol{h}} \cdot (\boldsymbol{z} \cdot \boldsymbol{e}^{00}_{200}(\boldsymbol{h}) \cdot \boldsymbol{z}).
\end{aligned} \tag{2.12}$$

They depend on the (local) macroscopic strain $\boldsymbol{h}$. They operate on the cross-sectional degrees of freedom $\boldsymbol{z}$ and $\boldsymbol{z}^\dagger$ (but not $\boldsymbol{z}^\ddagger$) and on the local values of the derivatives $\boldsymbol{h}^\dagger$ and $\boldsymbol{h}^\ddagger$ of the macroscopic strain.

As shown in Appendix A, the expansion of the energy $\Phi[\boldsymbol{h}, \boldsymbol{y}_{\boldsymbol{h}} + \boldsymbol{z}]$ in powers of the successive gradients of macroscopic strain can be expressed in terms of these operators as

$$\begin{aligned}
\Phi[\boldsymbol{h}, \boldsymbol{y}_{\boldsymbol{h}} + \boldsymbol{z}] = \int_0^L W_{\mathrm{hom}}(\boldsymbol{h}(S))\, \mathrm{d}S + \int_0^L \boldsymbol{A}_{\boldsymbol{h}(S)} \cdot \boldsymbol{h}'(S)\, \mathrm{d}S \cdots \\
+ [\boldsymbol{C}^{(0)}_{\boldsymbol{h}} \cdot \boldsymbol{h}' + \boldsymbol{C}^{(1)}_{\boldsymbol{h}} \cdot \boldsymbol{z}]^L_{S=0} + \int_0^L \left(\frac{1}{2}\, \boldsymbol{h}' \cdot \boldsymbol{B}^{(0)}_{\boldsymbol{h}} \cdot \boldsymbol{h}' + \boldsymbol{h}' \cdot \boldsymbol{B}^{(1)}_{\boldsymbol{h}} \cdot \boldsymbol{z} + \frac{1}{2}\, \boldsymbol{z} \cdot \boldsymbol{B}^{(2)}_{\boldsymbol{h}} \cdot \boldsymbol{z} \right)_S \mathrm{d}S \cdots \\
+ \mathcal{O}(|\boldsymbol{h}'|^3, |\boldsymbol{h}''||\boldsymbol{h}'|^2, |\boldsymbol{h}'''|).
\end{aligned} \tag{2.13}$$

In the boundary term in square brackets, both the arguments $\boldsymbol{h}$ in subscript of the operators and the operands $\boldsymbol{h}'$ and $\boldsymbol{z}$ must be evaluated at $S = 0$ and $S = L$, respectively. Likewise in the integrand on the second line, the quantities $\boldsymbol{h}$, $\boldsymbol{h}'$ and $\boldsymbol{z}$ must be evaluated at the current point S.

The form of the strain gradient model above is similar to that derived in different contexts, see for example in Bardenhagen and Triantafyllidis (1994); our main contribution is a method for calculating the coefficients $\boldsymbol{A}_{\boldsymbol{h}(S)}$, $\boldsymbol{B}^{(1)}_{\boldsymbol{h}}$, etc. explicitly.

2.5. Optimal correction

The last step in the reduction process is to determine the correction $\boldsymbol{z}(S)$ such that the microscopic displacement (2.8) satisfies the optimality condition (2.4). All derivatives of the unknown $\boldsymbol{z}(S)$ can be eliminated from equation (2.13), thanks to an integration by parts, as shown in Appendix A.5. The benefit is that the relaxation of the unknown $\boldsymbol{z}$ leads to a *local* problem in the cross-sections: as established in Appendix A, the optimal correction $\boldsymbol{z}(S)$ S is

$$\boldsymbol{z}(S) = \boldsymbol{z}_{\rm opt}(S) + \mathcal{O}(|\boldsymbol{h}'|^2),$$

where the dominant contribution $\boldsymbol{z}_{\rm opt} = \mathcal{O}(|\boldsymbol{h}'|)$ is the one that minimizes the local elastic potential $\boldsymbol{z} \mapsto \left(\frac{1}{2}\,\boldsymbol{h}'(S)\cdot\boldsymbol{B}^{(0)}_{\boldsymbol{h}(S)}\cdot\boldsymbol{h}'(S) + \boldsymbol{h}'(S)\cdot\boldsymbol{B}^{(1)}_{\boldsymbol{h}(S)}\cdot\boldsymbol{z} + \frac{1}{2}\,\boldsymbol{z}\cdot\boldsymbol{B}^{(2)}_{\boldsymbol{h}(S)}\cdot\boldsymbol{z}\right)$, subject to the constraint $\boldsymbol{q}(\boldsymbol{z}) = 0$. The correction $\boldsymbol{z}_{\rm opt}(S)$ is therefore the solution to the following variational problem,

$$\left\{\begin{array}{ll} \forall \hat{\boldsymbol{z}} & \boldsymbol{h}'(S)\cdot\boldsymbol{B}^{(1)}_{\boldsymbol{h}(S)}\cdot\hat{\boldsymbol{z}} + \boldsymbol{z}_{\rm opt}(S)\cdot\boldsymbol{B}^{(2)}_{\boldsymbol{h}(S)}\cdot\hat{\boldsymbol{z}} - \boldsymbol{f}_{\rm opt}(S)\cdot\boldsymbol{q}(\hat{\boldsymbol{z}}) = 0 \\ & \boldsymbol{q}\left(\boldsymbol{z}_{\rm opt}(S)\right) = \boldsymbol{0}, \end{array}\right. \tag{2.14}$$

where $\boldsymbol{f}_{\rm opt}(S)$ is a Lagrange multiplier, to be determined as part of the solution process.

This variational problem is linear with respect to the local value of the strain gradient $\boldsymbol{h}'(S)$. This implies that its solution $\boldsymbol{z}_{\rm opt}(S)$ is proportional to $\boldsymbol{h}'(S)$, i.e., there exists a catalog of corrections $\boldsymbol{Z}^{\boldsymbol{h}(S)}_{\rm opt}$ such that

$$\boldsymbol{z}_{\rm opt}(S) = \boldsymbol{Z}^{\boldsymbol{h}(S)}_{\rm opt}\cdot\boldsymbol{h}'(S). \tag{2.15}$$

The catalog $\boldsymbol{Z}^{\boldsymbol{h}}_{\rm opt}$ is found by solving (2.14). It can be determined once for all in terms of the geometric and mechanical properties of a reference cross-section and in terms of the macroscopic strain $\boldsymbol{h}$, as we show in the examples.

Equation (2.14) is a problem of linear elasticity in the cross-section. The first term $\boldsymbol{h}'(S)\cdot\boldsymbol{B}^{(1)}_{\boldsymbol{h}(S)}\cdot\hat{\boldsymbol{z}}$ can be interpreted as a pre-stress arising from the presence a gradient (an interpretation of this pre-stress term will be obtained based on the analysis of specific structures, see §5.4 in particular). The second term $\boldsymbol{z}_{\rm opt}(S)\cdot\boldsymbol{B}^{(2)}_{\boldsymbol{h}(S)}\cdot\hat{\boldsymbol{z}}$ is an elastic stiffness term which, in view of the definition of $\boldsymbol{B}^{(2)}_{\boldsymbol{h}(S)}$ in equation (2.12) has two contributions: a tangent elastic stiffness $\boldsymbol{K}_{\boldsymbol{h}(S)}$, and a geometric stiffness arising from the pre-stress $\boldsymbol{\Sigma}_{\boldsymbol{h}(S)}$ associated with the local state of stress.

2.6. Relaxed energy

The relaxed energy $\Phi^\star[\boldsymbol{h}]$ is finally obtained by inserting the optimal displacement $\boldsymbol{y}(S) = \boldsymbol{y}_{\boldsymbol{h}(S)} + \boldsymbol{z}_{\rm opt}(S) + \cdots$ into the energy expansion in equation (2.13). The result is

$$\Phi^\star[\boldsymbol{h}] = \int_0^L W_{\rm hom}(\boldsymbol{h}(S))\,{\rm d}S + \int_0^L \boldsymbol{A}_{\boldsymbol{h}(S)}\cdot\boldsymbol{h}'(S)\,{\rm d}S + \left[\boldsymbol{C}_{\boldsymbol{h}(S)}\cdot\boldsymbol{h}'(S)\right]_0^L + \frac{1}{2}\int_0^L \boldsymbol{h}'(S)\cdot\boldsymbol{B}_{\boldsymbol{h}(S)}\cdot\boldsymbol{h}'(S)\,{\rm d}S + \ldots \tag{2.16}$$

Here, the operator $\boldsymbol{A}_{\boldsymbol{h}}$ has been introduced in equation (2.12) and the additional elastic moduli $\boldsymbol{B}_{\boldsymbol{h}}$ and $\boldsymbol{C}_{\boldsymbol{h}}$ are defined by

$$\begin{array}{rcl} \boldsymbol{B}_{\boldsymbol{h}} & = & \boldsymbol{B}^{(0)}_{\boldsymbol{h}} - \left(\boldsymbol{Z}^{\boldsymbol{h}}_{\rm opt}\right)^T\cdot\boldsymbol{B}^{(2)}_{\boldsymbol{h}}\cdot\boldsymbol{Z}^{\boldsymbol{h}}_{\rm opt}, \\ \boldsymbol{C}_{\boldsymbol{h}} & = & \boldsymbol{C}^{(0)}_{\boldsymbol{h}} + \boldsymbol{C}^{(1)}_{\boldsymbol{h}}\cdot\boldsymbol{Z}^{\boldsymbol{h}}_{\rm opt}. \end{array} \tag{2.17}$$

The energy functional in equation (2.16) and the explicit expression for the strain-gradient modulus $\boldsymbol{B}_{\boldsymbol{h}}$ are the main results of this paper.

In equation (2.16), the leading order term in the expansion depends $W_{\rm hom}$, and defines structural models without the gradient effect, see § 2.3. The second term depending on $\boldsymbol{A}_{\boldsymbol{h}}$ yields an energy contribution that is linear with respect to the gradient $\boldsymbol{h}'$: it is zero in most cases due to symmetry reasons, as shown in the

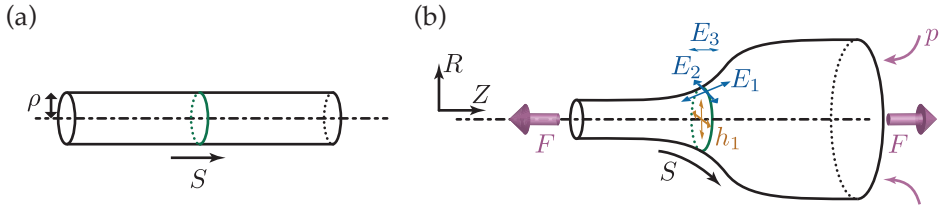

Figure 3: An axisymmetric membrane: (a) reference and (b) current configurations.

forthcoming examples. The terms depending on $\boldsymbol{C}_{\boldsymbol{h}}$ is a boundary term arising from a gradient effect, while the last term is the bulk strain-gradient term.

For further reference, we note that the strain gradient term is available in alternative form as

$$\frac{1}{2}\int_0^L \boldsymbol{h}'(S)\cdot\boldsymbol{B}_{\boldsymbol{h}(S)}\cdot\boldsymbol{h}'(S)\,\mathrm{d}S = \frac{1}{2}\int_0^L \boldsymbol{h}'(S)\cdot\boldsymbol{B}^{(0)}_{\boldsymbol{h}(S)}\cdot\boldsymbol{h}'(S)\,\mathrm{d}S - \frac{1}{2}\int_0^L \boldsymbol{z}_{\mathrm{opt}}\cdot\boldsymbol{B}^{(2)}_{\boldsymbol{h}}\cdot\boldsymbol{z}_{\mathrm{opt}}\,\mathrm{d}S.$$

2.7. A necessary stability condition at the microscopic scale

A necessary condition for the microscopic correction derived in section 2.5 to be stable (and, hence, for the relaxed energy $\Phi^\star$ to be meaningful) is that the stiffness operator $\boldsymbol{B}^{(2)}_{\boldsymbol{h}}$ appearing in the microscopic problem in equation (2.14) is non-negative,

$$(\forall \boldsymbol{z} \text{ such that } \boldsymbol{q}(\boldsymbol{z})=\boldsymbol{0}) \quad \boldsymbol{z}\cdot\boldsymbol{B}^{(2)}_{\boldsymbol{h}}\cdot\boldsymbol{z}\geq 0. \tag{2.18}$$

Note that this condition does not warrant that the matrix $\boldsymbol{B}_{\boldsymbol{h}}$ of strain-gradient moduli is non-negative, see equation (2.17) (a matrix $\boldsymbol{B}_{\boldsymbol{h}}$ having negative eigenvalues is indeed obtained for the elastic block, see §4.7). However, equation (2.18) does warrant

$$\frac{1}{2}\boldsymbol{h}'(S)\cdot\boldsymbol{B}_{\boldsymbol{h}(S)}\cdot\boldsymbol{h}'(S)\leq\frac{1}{2}\boldsymbol{h}'(S)\cdot\boldsymbol{B}^{(0)}_{\boldsymbol{h}}\cdot\boldsymbol{h}'(S),$$

which, as discussed in section 6, shows that our 1d model relaxes the elastic energy better than strain gradient models derived from the *ad hoc* kinematic assumption $\boldsymbol{z}(S)=\boldsymbol{0}$: this benefit is a consequence of the fact that our 1d model is asymptotically exact.

3. Application to an axisymmetric membrane

Upon inflation, axisymmetric rubber membranes feature localized deformations in the form of propagating bulges (Kyriakides and Chang, 1991). Standard dimension reduction without gradient terms yields a non-convex elastic potential W_{hom} and thus fails at describing the details of localization. Localized solutions can be analyzed using the full membrane model (Fu et al., 2008; Pearce and Fu, 2010), but are more easily and very accurately described based on a 1d strain-gradient model, as recently shown by the authors, starting from the theory of axisymmetric elastic membranes and using a typical constitutive law for rubber (Lestringant and Audoly, 2018). This 1d model is rederived here as a first illustration of the general reduction method presented in section 2.

3.1. Full axisymmetric membrane model

The reference configuration is chosen as the natural, cylindrical configuration of the membrane, and the natural radius of the circular membrane is denoted by ρ. In the current configuration, the membrane is deformed under the action of an inflating pressure p, and a pulling force F equally distributed over the terminal cross-sections, see figure 3. Natural boundary conditions are used, i.e., there is no restraint on the terminal cross-sections.

An axisymmetric configuration of the membrane is parameterized by two functions $Z(S)$ and $R(S)$, such that the cross-section with arc-length coordinate S in the reference configuration is transformed into a circle perpendicular to the axis of the shell, with axial coordinate $Z(S)$ and radius $R(S)$, see figure 3(b). We consider a standard set of strain measures from the theory of finite-strain axisymmetric elasticity, $\boldsymbol{E} = \left(\begin{array}{c|c|c} \sqrt{Z'^2 + R'^2} & \frac{R}{\rho} & Z' \end{array} \right)$: $E_1 = \sqrt{Z'^2 + R'^2}$ and $E_2 = \frac{R}{\rho}$, usually denoted as $(E_1, E_2) = (\lambda_S, \lambda_\Theta)$, are the membrane stretches in the (principal) longitudinal and circumferential directions, respectively. The additional 'strain' E_3 has been included for convenience, as it allows us to write the potential energy of the pulling force F as $-F\,[Z(S)]_0^L = -F\int_0^L E_3\,\mathrm{d}S$.

The sum of the membrane strain energy, and the potential energy of the loads p and F is captured by an effective potential $W(\boldsymbol{E})$ per unit length $\mathrm{d}S$,

$$W(\boldsymbol{E}) = \overline{W}(E_1, E_2) - p\,\pi\,\rho^2\,E_2^2\,E_3 - F\,E_3,$$

where $\overline{W}(E_1, E_2) = \overline{W}(\lambda_S, \lambda_\Theta)$ is the strain energy of the hyperelastic membrane model (we use bars generally for quantities relating to the full model). Upon integration with respect to S, the second term yields $(-p)$ times the volume enclosed by the membrane, which is the potential energy of the pressure force. Note that we have chosen to include the potential energy of the loads p and F into the potential $\Phi = \int_0^L W\,\mathrm{d}S$ which normally captures the strain energy only; in line with this, the loading parameters p and F are considered constant.

3.2. Macroscopic and microscopic variables

A natural choice of macroscopic strain parameter is the apparent axial stretch $Z'(S)$: this is the stretch of a virtual bar obtained by collapsing all the circular cross-sections to a point located at their center. However, this choice has the drawback that, for typical constitutive laws for rubber, there can be several homogeneous solutions corresponding to a given value of the apparent stretch. To work around this difficulty, it is preferable to define instead the macroscopic strain parameter as the hoop stretch $h_1(S) = E_2(S) = \frac{R(S)}{\rho}$. As we will see, it is possible to reconstruct the apparent axial stretch $Z'(S)$ in terms of this $h_1(S)$. We thus apply the general formalism using a single macroscopic strain and a single microscopic degree of freedom, defined as

$$\boldsymbol{h}(S) = (h_1(S)) = \left(\frac{R(S)}{\rho}\right), \quad \boldsymbol{y}(S) = (y_1(S)) = (Z'(S)).$$

With this choice of macroscopic and microscopic variables, it is possible to reconstruct the configuration using $R(S) = \rho\,h_1(S)$ and $Z(S) = Z(0) + \int_0^S y_1(\overline{S})\,\mathrm{d}\overline{S}$, where $Z(0)$ is an unimportant rigid-body translation. As we do not need any constraint for this particular structural model, we set $\boldsymbol{q}(\boldsymbol{y}) = ()$ and drop all the terms containing $\boldsymbol{q}(\boldsymbol{y})$ in the general formalism.

The strain vector $\boldsymbol{E}$ for the axisymmetric membrane given in section 3.1 can be cast in the canonical form from equation (2.1) by choosing the strain function as

$$\boldsymbol{E}(\boldsymbol{h}, \boldsymbol{h}^\dagger; \boldsymbol{y}, \boldsymbol{y}^\dagger, \boldsymbol{y}^\ddagger) = \left(\begin{array}{c|c|c} \sqrt{\rho^2\,h_1^{\dagger 2} + y_1^2} & h_1 & y_1 \end{array} \right),$$

where the arguments are vectors whose length matches that of the macroscopic strain $\boldsymbol{h}$ and microscopic variable $\boldsymbol{y}$ proposed above, i.e., $\boldsymbol{h} = (h_1)$, $\boldsymbol{h}^\dagger = (h_1^\dagger)$, $\boldsymbol{y} = (y_1)$, $\boldsymbol{y}^\dagger = (y_1^\dagger)$ and $\boldsymbol{y}^\ddagger = (y_1^\ddagger)$.

3.3. Homogeneous solutions

Homogeneous solutions are first analyzed, by setting to zero the derivative terms in the definition of the strain, see equation (2.5). This yields the homogeneous strain as

$$\tilde{\boldsymbol{E}}(\boldsymbol{h}, \boldsymbol{y}) = \left(\begin{array}{c|c|c} y_1 & h_1 & y_1 \end{array} \right).$$

The generalized stress in the homogeneous solution is given by the gradient of the potential $\boldsymbol{E}(S)$,

$$\frac{\mathrm{d}W}{\mathrm{d}E}(\tilde{\boldsymbol{E}}(\boldsymbol{h}, \boldsymbol{y})) = \left(\begin{array}{c|c|c} \overline{\Sigma}_S(y_1, h_1) & \overline{\Sigma}_\Theta(y_1, h_1) - 2\,p\,\pi\,\rho^2\,h_1\,y_1 & -F - p\,\pi\,\rho^2\,h_1^2 \end{array} \right),$$

where $\overline{\Sigma}_S(\lambda_S,\lambda_\Theta)=\frac{\partial\overline{W}}{\partial\lambda_S}(\lambda_S,\lambda_\Theta)$ and $\overline{\Sigma}_\Theta(\lambda_S,\lambda_\Theta)=\frac{\partial\overline{W}}{\partial\lambda_\Theta}(\lambda_S,\lambda_\Theta)$ are the components of the Piola-Kirchhoff stress in the longitudinal and circumferential directions, respectively, as predicted by the elastic strain potential $\overline{W}(\lambda_S,\lambda_\Theta)$ characterizing the elastic properties of the membrane.

Next, we proceed to write and solve the principle of virtual work (2.6) for homogeneous solutions. Noting that $\frac{\partial\tilde{\boldsymbol{E}}}{\partial\boldsymbol{y}}(\boldsymbol{h},\boldsymbol{y})=\left(\begin{array}{c|c|c} 1 & 0 & 1 \end{array}\right)$, it writes

$$-\overline{\Sigma}_S(y_1^{(h_1)},h_1)+F+p\,\pi\,\rho^2\,h_1^2=0. \tag{3.1}$$

This is an equation for the longitudinal stretch $y_1^{(h_1)}$ in a homogeneous solution, in terms of the hoop stretch $h_1=\frac{R}{\rho}$. The load parameters F and ρ are considered fixed, i.e., the dependence on F and ρ will always be silent. Equation (3.1) expresses the equilibrium of a homogeneous solution in the longitudinal direction. For typical constitutive laws, equation (3.1) cannot be solved explicitly for $y_1^{(h_1)}$ in terms of h_1, and will be viewed as an implicit equation.

In terms of the homogeneous solution $y_1^{(h_1)}$, we obtain the properties of homogeneous solution from equation (2.7) as

$$\begin{array}{lcl}
\boldsymbol{E}_{(h_1)} & = & \left(\begin{array}{c|c|c} y_1^{(h_1)} & h_1 & y_1^{(h_1)} \end{array}\right)\\
W_{\rm hom}(h_1) & = & \overline{W}(y_1^{(h_1)},h_1)-\overline{\Sigma}_S(y_1^{(h_1)},h_1)\,y_1^{(h_1)}\\
\boldsymbol{\Sigma}_{(h_1)} & = & \left(\begin{array}{c|c|c} \overline{\Sigma}_S(y_1^{(h_1)},h_1) & * & -\overline{\Sigma}_S(y_1^{(h_1)},h_1) \end{array}\right)\\
\boldsymbol{K}_{(h_1)} & = & \left(\begin{array}{ccc} \overline{K}_{SS}(y_1^{(h_1)},h_1) & * & 0\\ * & * & *\\ 0 & * & 0 \end{array}\right).
\end{array} \tag{3.2}$$

Here, the star symbol $(*)$ denote quantities that play no role and do not need to be calculated. The quantity $\overline{K}_{SS}(\lambda_S,\lambda_\Theta)=\frac{\partial^2\overline{W}}{(\partial\lambda_S)^2}(\lambda_S,\lambda_\Theta)$ is the tangent elastic modulus, as calculated from the membrane model.

3.4. Change of microscopic variable

According to the general method, we introduce a correction $\boldsymbol{z}(S)=(z_1(S))$ to the microscopic variable by $\boldsymbol{y}(S)=\boldsymbol{y}_{\boldsymbol{h}}(S)+\boldsymbol{z}(S)$, i.e., $y_1(S)=y_1^{(h_1(S))}+z_1(S)$. In terms of the new unknown, the strain function reads, see equation (2.9),

$$\boldsymbol{e}_{\boldsymbol{h}}(\boldsymbol{h}^\dagger,\boldsymbol{h}^\ddagger;\boldsymbol{z},\boldsymbol{z}^\dagger,\boldsymbol{z}^\ddagger)=\left(\begin{array}{c|c|c} \sqrt{\rho^2\,h_1^{\dagger 2}+(y_1^{(h_1)}+z_1)^2} & h_1 & y_1^{(h_1)}+z_1 \end{array}\right),$$

where again the arguments are vectors whose dimension is imposed by the macroscopic strain and microscopic variable as $\boldsymbol{h}^\dagger=(h_1^\dagger)$, $\boldsymbol{h}^\ddagger=(h_1^\ddagger)$, $\boldsymbol{z}=(z_1)$, $\boldsymbol{z}^\dagger=(z_1^\dagger)$ and $\boldsymbol{z}^\ddagger=(z_1^\ddagger)$. Note that the strain function $\boldsymbol{e}_{\boldsymbol{h}}=\boldsymbol{e}_{(h_1)}$ depends on the macroscopic strain h_1 which appears in subscript, and that we have made use of the catalog of homogeneous solutions $y_1^{(h_1)}$ in the right-hand side.

The structure coefficients $\boldsymbol{e}^{ij}_{klm}(\boldsymbol{h})$ are the successive partial derivatives of the right-hand side above, see equation (2.11). These partial derivatives are most easily found by identifying $\boldsymbol{e}_{\boldsymbol{h}}(\boldsymbol{h}^\dagger,\boldsymbol{h}^\ddagger;\boldsymbol{z},\boldsymbol{z}^\dagger,\boldsymbol{z}^\ddagger)$ with its Taylor expansion $\left(\begin{array}{c|c|c} y_1^{(h_1)}+z_1+\frac{\rho^2\,h_1^{\dagger 2}}{2\,y_1^{(h_1)}} & h_1 & y_1^{(h_1)}+z_1 \end{array}\right)$. The result is

$$\begin{array}{c}
\boldsymbol{e}^{10}_{000}(\boldsymbol{h})=\boldsymbol{0}\quad \boldsymbol{e}^{20}_{000}(\boldsymbol{h})=\left(\begin{array}{c|c|c} \frac{\rho^2}{y_1^{(h_1)}} & 0 & 0 \end{array}\right)\quad \boldsymbol{e}^{01}_{000}(\boldsymbol{h})=\boldsymbol{0}\quad \boldsymbol{e}^{10}_{100}(\boldsymbol{h})=\boldsymbol{0}\\
\boldsymbol{e}^{00}_{100}(\boldsymbol{h})=\left(\begin{array}{c|c|c} 1 & 0 & 1 \end{array}\right)\quad \boldsymbol{e}^{00}_{200}(\boldsymbol{h})=\boldsymbol{0}\quad \boldsymbol{e}^{00}_{010}(\boldsymbol{h})=\boldsymbol{0}.
\end{array} \tag{3.3}$$

These are the only structure coefficients that are required in the following. Recall that the dimension of both $\boldsymbol{h}$ and $\boldsymbol{y}$ is one for an axisymmetric membrane: the tensors $\boldsymbol{e}^{ij}_{klm}$, which are of dimensions $3\times1\times\cdots\times1$ according to the general rule, where the one's are repeated $i+j+k+l+m$ times, have been identified with vectors of dimension 3.

When these expressions are combined with those for homogeneous quantities obtained in (3.2), one can calculate the first batch of operators from equation (2.12) as

$$\begin{aligned}
\boldsymbol{A_h}\cdot\boldsymbol{h}^\dagger &= \boldsymbol{\Sigma_h}\cdot(\boldsymbol{e}^{10}_{000}(\boldsymbol{h})\cdot\boldsymbol{h}^\dagger)=\boldsymbol{\Sigma_h}\cdot\boldsymbol{0}=0\\
\boldsymbol{C}^{(0)}_{\boldsymbol{h}}\cdot\boldsymbol{h}^\ddagger &= \boldsymbol{\Sigma_h}\cdot(\boldsymbol{e}^{01}_{000}(\boldsymbol{h})\cdot\boldsymbol{h}^\ddagger)=\boldsymbol{\Sigma_h}\cdot\boldsymbol{0}=0\\
\boldsymbol{C}^{(1)}_{\boldsymbol{h}}\cdot\boldsymbol{z}^\dagger &= \boldsymbol{\Sigma_h}\cdot(\boldsymbol{e}^{00}_{010}(\boldsymbol{h})\cdot\boldsymbol{z}^\dagger)=\boldsymbol{\Sigma_h}\cdot\boldsymbol{0}=0\\
\tfrac{1}{2}\,\boldsymbol{h}^\dagger\cdot\boldsymbol{B}^{(0)}_{\boldsymbol{h}}\cdot\boldsymbol{h}^\dagger &= \tfrac{1}{2}\,\boldsymbol{0}\cdot\boldsymbol{K_h}\cdot\boldsymbol{0}+\tfrac{1}{2}\,\boldsymbol{\Sigma_h}\cdot\Big(\begin{array}{c|c|c}\frac{\rho^2}{y_1^{(h_1)}}\,(h_1^\dagger)^2 & 0 & 0\end{array}\Big)-\boldsymbol{h}^\dagger\cdot\boldsymbol{0}\cdot\boldsymbol{h}^\dagger=\tfrac{1}{2}\,\overline{\Sigma}_S(y_1^{(h_1)},h_1)\,\tfrac{\rho^2}{y_1^{(h_1)}}\,(h_1^\dagger)^2\\
\boldsymbol{h}^\dagger\cdot\boldsymbol{B}^{(1)}_{\boldsymbol{h}}\cdot\boldsymbol{z} &= \boldsymbol{0}\cdot\boldsymbol{K_h}\cdot(*)+\boldsymbol{\Sigma_h}\cdot\boldsymbol{0}-\boldsymbol{h}^\dagger\cdot\boldsymbol{0}\cdot\boldsymbol{z}=0\\
\tfrac{1}{2}\,\boldsymbol{z}\cdot\boldsymbol{B}^{(2)}_{\boldsymbol{h}}\cdot\boldsymbol{z} &= \tfrac{1}{2}\,\Big(\begin{array}{c|c|c}1&0&1\end{array}\Big)\cdot\boldsymbol{K_h}\cdot\Big(\begin{array}{c|c|c}1&0&1\end{array}\Big)+\tfrac{1}{2}\,\boldsymbol{\Sigma_h}\cdot\boldsymbol{0}=\tfrac{1}{2}\,\overline{K}_{SS}(y_1^{(h_1)},h_1)\,(z_1)^2.
\end{aligned}$$

3.5. Local optimization problem

The local optimization problem (2.14) is particularly simple, because it has no source term ($\boldsymbol{B}^{(1)}_{\boldsymbol{h}}=\boldsymbol{0}$) and no constraint term ($\boldsymbol{q}(\boldsymbol{y})=()$). In view of the operators just derived, it reads

$$\forall\hat{z}_1\quad \hat{z}_1\,\overline{K}_{SS}(y_1^{(h_1)},h_1)\,z_1^{\text{opt}}=0.$$

We rule out the possibility of a material instability in the membrane model, i.e., $\overline{K}_{SS}(y_1^{(h_1)},h_1)>0$ (note that with this assumption of material stability at the 'microscopic' level, the stability condition from section 2.7 is automatically satisfied). The variational problem above can then be solved for $\boldsymbol{z}_{\text{opt}}=\big(z_1^{\text{opt}}\big)$ as $\boldsymbol{z}_{\text{opt}}(\tilde{S})=\boldsymbol{0}$. The correction to the microscopic variable arising from the gradient effect is zero for this particular structure. To comply with the general form of equation (2.15), we set accordingly $\boldsymbol{Z}^{\boldsymbol{h}}_{\text{opt}}=\Big(\begin{array}{c}0\end{array}\Big)$.

3.6. Regularized model

In view of equation (2.17), we obtain the operators entering into the strain-gradient model as $\boldsymbol{A_h}=\boldsymbol{0}$, $\boldsymbol{B_h}=(B^{(h_1)}_{11})$ where $B^{(h_1)}_{11}=\frac{\rho^2\,\overline{\Sigma}_S(y_1^{(h_1)},h_1)}{y_1^{(h_1)}}$ and $\boldsymbol{C_h}=\boldsymbol{0}$.

We switch to the more standard notation $\lambda_\Theta=h_1=\frac{R}{\rho}$ for the hoop stretch and $\lambda_S=y_1$ for the apparent axial stretch, and recapitulate the main results for the axisymmetric membrane as follows. We must first solve the implicit equation (3.1) for the apparent axial stretch $y_1^{(h_1)}=\lambda_S^{\text{hom}}(\lambda_\Theta)$, which reads $\overline{\Sigma}_S\big(\lambda_S^{\text{hom}}(\lambda_\Theta),\lambda_\Theta\big)=F+p\,\pi\,\rho^2\,\lambda_\Theta^2$ and yields the homogeneous equilibria of the balloon. In this equation, $\overline{\Sigma}_\Theta(\lambda_S,\lambda_\Theta)=\frac{\partial\overline{W}}{\partial\lambda_\Theta}(\lambda_S,\lambda_\Theta)$ is the hoop stress in the homogeneous solution. In terms of this catalog of homogeneous solutions, we can calculate $W_{\text{hom}}(\lambda_\Theta)$ by (3.2). The balloon is governed by the strain-gradient bar model, see equation (2.16),

$$\Phi^\star[\lambda_\Theta]\approx\int_0^L\left[W_{\text{hom}}(\lambda_\Theta(S))+\frac{1}{2}\,B(\lambda_\Theta(S))\,\lambda_\Theta'^2(S)\right]\mathrm{d}S,\tag{3.4a}$$

where the strain-gradient modulus reads

$$B(\lambda_\Theta)=\frac{\rho^2\,\overline{\Sigma}_S\big(\lambda_S^{\text{hom}}(\lambda_\Theta),\lambda_\Theta\big)}{\lambda_S^{\text{hom}}},\tag{3.4b}$$

and where $\overline{\Sigma}_S(\lambda_S,\lambda_\Theta)=\frac{\partial\overline{W}}{\partial\lambda_S}(\lambda_S,\lambda_\Theta)$ is the longitudinal stress in the homogeneous solution.

3.7. Comments

We have recovered the model established by Lestringant and Audoly (2018). Typical solutions predicted by the 1d model are compared to those of the full axisymmetric model in figure 4: the 1d models appears to be highly accurate, even in the regime where the bulges are fully localized.

The axisymmetric membrane model, which we used as a starting point was already a 1d model: it does not make use of any transverse variable, and has discrete degrees of freedom (Z,R) in each cross-section. The

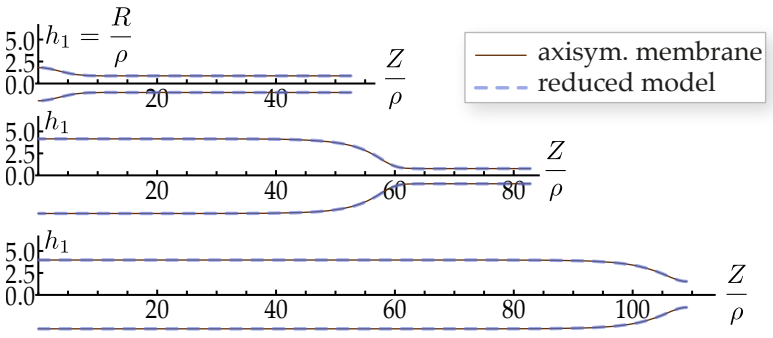

Figure 4: Solutions for a propagating bulge in an axisymmetric membrane with initial aspect ratio $L/\rho = 30$: comparison of the predictions of the full axisymmetric membrane model (§3.1) and of the reduced model in equation (3.4), from Lestringant and Audoly (2018). The material model for rubber proposed by Ogden (1972) is used, with the same set of material parameters as used in the previous experimental work of Kyriakides and Chang (1991), see also §2 in Lestringant and Audoly (2018).

reduction method led us to another 1d model and it therefore is improper to speak of dimension reduction in this case. The reduction method is still useful, as reduced model is simpler and, more importantly, much more standard: it is the well-known diffuse-interface model introduced by van der Walls in the context of liquid-vapor phase transition, as discussed by by Lestringant and Audoly (2018).

Even when bulges are fully formed, the typical length of the interface between the bulged and unbulged regions never gets much less than $\sim \rho$, i.e., remains always much larger than than the membrane's thickness t (assuming the membrane is thin in a first place $\rho \gg t$). This warrants that the assumptions underlying the membrane model remain valid. To address the case of thick membranes, i.e., when the ratio t/ρ is not small, one could apply our reduction method to a theory of thick membranes, or to a finite-strain model for a hyperelastic cylinder in 3d.

4. Application to a linearly elastic block

Our next example is a homogeneous block of linearly elastic material in 2d, having length L and thickness a, as sketched in figure 5. We account for both stretching and bending of the block. In the first step of the dimension reduction, we will recover the classical beam model. Its energy is convex, implying that this particular structure does not tend to localize. The strain-gradient model obtained at the next step is still of interest as its solutions generally [2] converge faster towards those of the full (2d) elasticity model than those of the classical beam model.

There is a large amount of work on higher-order asymptotic expansions for prismatic solids in the specific context of linear elasticity with the aim to derive *linear* higher-order beam theories, see for instance the work of Trabucho and Viaño (1996). The forthcoming analysis shows that these results can be easily recovered with our method. It also reveals that the assumption of linear elasticity brings in severe, somewhat hidden limitations.

The elastic block is our first example where a cross-section possesses infinitely many degrees of freedom.

4.1. Full model: a linearly elastic block in 2d

We consider an elastic block in reference configuration. The axial and transverse coordinates in reference configuration are denoted as S and T, respectively, and are used as Lagrangian coordinates. Their domains are $0 \leq S \leq L$ and $-a/2 \leq T \leq a/2$.

[2] It is known, however, that boundary conditions can prevent strain-gradient models from converging faster. This happens when the imposed boundary conditions are incompatible with the kinematics $\boldsymbol{y}(S) = \boldsymbol{y}_{\text{hom}}(\boldsymbol{h}(S)) + \boldsymbol{z}_{\text{opt}} + \cdots$ of the strain-gradient model at the microscopic scale. We do not address this question in this paper, and limit attention to natural boundary conditions.

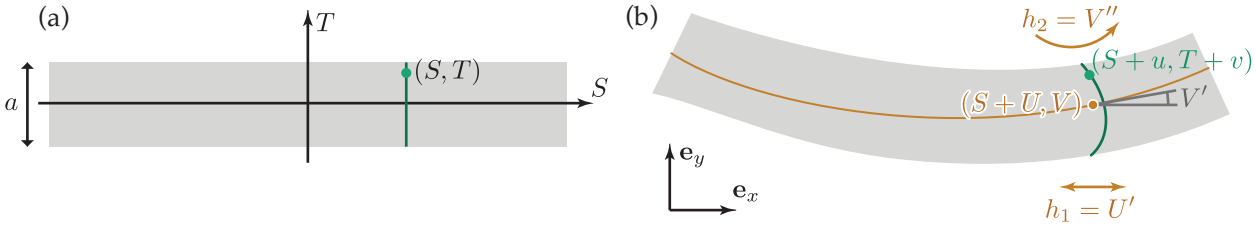

Figure 5: A block of a linearly elastic material in (a) reference and (b) current configuration. The 1d model makes use of the center line (brown curve), defined as the curve passing through the centers of mass (brown dots) of the cross-section. The macroscopic strain are the apparent stretch $h_1(S) = U'(S)$ and the apparent curvature $h_2(S) = V''(S)$ of the center line.

We introduce the displacement (u, v) in a Cartesian frame $(\boldsymbol{e}_x, \boldsymbol{e}_y)$ aligned with axes of the undeformed block: a point with position (S, T) in reference configuration gets mapped to $\boldsymbol{x}(S, T) = (S + u(S, T), T + v(S, T))$ in the current configuration, see figure 5(b). The linear strain is presented in vector form as

$$\boldsymbol{E} = \left(\begin{array}{c|c|c} \frac{\partial u}{\partial S} & \frac{\partial v}{\partial T} & \frac{1}{2}\left(\frac{\partial u}{\partial T} + \frac{\partial v}{\partial S}\right) \end{array} \right) \tag{4.1}$$

where E_1, E_2 and E_3 are respectively the SS, TT and ST components of the 2-d strain tensor from linear elastic theory. We use a linear isotropic and uniform constitutive in 2d (Hookean elasticity), corresponding to an elastic potential per unit length dS

$$W(\boldsymbol{E}) = \frac{1}{2} \int_{-a+2}^{+a/2} (2\,\mu\,(E_1^2 + E_2^2 + 2\,E_3^2) + \lambda\,(E_1 + E_2)^2)\,\mathrm{d}T, \tag{4.2}$$

where the elastic constants μ and λ are known as the Lamé parameters.

4.2. Macroscopic and microscopic variables

We choose to define the center line as the curve passing through the centers of mass of the cross-sections. The components of the center line displacement are therefore

$$U(S) = \langle u \rangle(S) \quad V(S) = \langle v \rangle(S), \tag{4.3}$$

where $\langle f \rangle(S) = \frac{1}{a} \int_{-a/2}^{+a/2} f(S, T)\,\mathrm{d}T$ denotes the cross-section average of a function $f(S, T)$.

The deformed center line is parametrized as $(S + U(S))\,\boldsymbol{e}_x + V(S)\,\boldsymbol{e}_y$. In the theory of linear elasticity, it is associated with an apparent longitudinal strain $U'(S)$, deflection angle $V'(S)$, and curvature $V''(S)$, where by 'apparent' we emphasize the fact that the center line is non-material. In our reduction of the elastic block to a 1d model, we use as macroscopic strain measures these apparent axial strain and curvature,

$$\boldsymbol{h}(S) = (U'(S), V''(S)).$$

Let $\tilde{\boldsymbol{x}}(S, T)$ the final position of the point initially at position $S\,\boldsymbol{e}_x + T\,\boldsymbol{e}_y$ if the cross-section S were to undergo a rigid body motion following the center line, namely the combination of a rigid-body translation $(U(S)\,\boldsymbol{e}_x + V(S)\,\boldsymbol{e}_y)$ and a rigid-body rotation with angle $V'(S)$. Since $V'(S)$ is infinitesimal, the unit normal to the center line writes $-V'(S)\,\boldsymbol{e}_x + \boldsymbol{e}_y$ and so $\tilde{\boldsymbol{x}}(S, T) = [(S + U(S))\,\boldsymbol{e}_x + V(S)\,\boldsymbol{e}_y] + T\,[-V'(S)\,\boldsymbol{e}_x + \boldsymbol{e}_y]$.

We choose to define the microscopic displacement $\boldsymbol{y}(S, T)$ as the difference between the actual position $\boldsymbol{x}(S, T) = (S + u(S, T))\,\boldsymbol{e}_x + (T + v(S, T))\,\boldsymbol{e}_y$ and $\tilde{\boldsymbol{x}}(S, T)$:

$$\boldsymbol{y}(S, T) = \boldsymbol{x}(S, T) - \tilde{\boldsymbol{x}}(S, T) = (u(S, T) - U(S) + V'(S)\,T)\,\boldsymbol{e}_x - (v(S, T) - V(S))\,\boldsymbol{e}_y.$$

The Cartesian components are found as $y_1(S, T) = u(S, T) - U(S) + V'(S)\,T$ and $y_2(S, T) = v(S, T) - V(S)$. This definition of $\boldsymbol{y}$ warrants $\boldsymbol{y}(S, T) = \boldsymbol{0}$ automatically whenever the block is moved rigidly, since $\boldsymbol{x}(S, T) = \tilde{\boldsymbol{x}}(S, T)$ in this case.

In our general presentation of the method in section 2, $\boldsymbol{y}(S)$ (with a single argument) was defined as the *collection* of the microscopic degrees of freedom on a given cross-section S. To comply with this convention, we define $\boldsymbol{y}(S) = (y_1(S), y_2(S))$ as a pair of *functions defined on the cross-section* taking the transverse coordinate T as an argument,

$$\begin{array}{rcl} y_1(S) & = & \{(u(S,T) - U(S) + V'(S)\,T)\}_T \\ y_2(S) & = & \{v(S,T) - V(S)\}_T. \end{array}$$

We recall that $\{g(T)\}_T$ is a notation for the function g that maps T to $g(T)$, the index T appearing in subscript after a curly brace being a dummy variable.

In view of equation (4.3), the microscopic displacement must satisfy the condition $\langle u\rangle(S) = U(S)$ and $\langle v\rangle(S) = V(S)$. Upon elimination of (u, v) in favor of (y_1, y_2), this yields $\langle y_1(S)\rangle = \langle y_2(S)\rangle = 0$ for all S. We handle these constraints by setting

$$\boldsymbol{q}(\boldsymbol{y}) = \frac{1}{a}\left(\int_{-a/2}^{a/2} y_1(T)\,\mathrm{d}T, \int_{-a/2}^{a/2} y_2(T)\,\mathrm{d}T\right)$$

in the general formalism of section 2.

The displacement in the Cartesian basis is $u(S,T) = U(S) + [y_1(S)](T) - V'(S)\,T$ and $v(S,T) = [y_2(S)](T) + V(S)$, and therefore the strain in equation (4.1) can be expressed as

$$\boldsymbol{E}(S) = \left(\ h_1(S) + [y_1'(S)](T) - h_2(S)\,T \ \middle|\ \partial_T[y_2(S)](T) \ \middle|\ \tfrac{1}{2}\left(\partial_T[y_1(S)](T) + [y_2'(S)](T)\right)\ \right).$$

Since primes are reserved for derivatives with respect to the longitudinal variable S, we use the symbol ∂_T for transverse derivatives.

In the above expression, $y_1'(S)$ denotes the function $\{y_1'(S,T)\}_T$, and similarly $y_2'(S) = \{y_2'(S,T)\}_T$. For consistency with the discrete case, we define the strain function $\boldsymbol{E}(\ldots)$ as an operator that takes as arguments the pair of *functions* $\boldsymbol{y} = \boldsymbol{y}(S) = (y_1(S), y_2(S))$, and their derivatives $\boldsymbol{y}^\dagger = \boldsymbol{y}'(S)$, as well as the pair of scalars $\boldsymbol{h}(S) = (h_1(S), h_2(S))$, and returns the strain *map* in the cross-section,

$$\boldsymbol{E}(\boldsymbol{h}, \boldsymbol{h}^\dagger, \boldsymbol{y}, \boldsymbol{y}^\dagger, \boldsymbol{y}^\ddagger) = \left(\ \{h_1 + y_1^\dagger(T) - h_2\,T\}_T \ \middle|\ \{\partial_T y_2(T)\}_T \ \middle|\ \left\{\tfrac{1}{2}\left(\partial_T y_1(T) + y_2^\dagger(T)\right)\right\}_T\ \right). \tag{4.4}$$

We use the same ordering conventions for the strain components as in equation (4.1), i.e. the longitudinal, transverse and shear strain appear in this order. We continue to use the same notation as earlier whereby variables bearing a dagger, such as $\boldsymbol{h}^\dagger = (h_1^\dagger, h_2^\dagger)$ are dummy variables that are intended to hold the local value of the derivative, here $\boldsymbol{h}'(S)$.

4.3. Homogeneous solutions

In the homogeneous case, the arguments of $\boldsymbol{E}$ corresponding to axial gradients in (4.4) (thus, bearing a single or a double dagger) are all set to zero, see equation (2.5). Doing so, we are left with the map of homogeneous strain,

$$\tilde{\boldsymbol{E}}(\boldsymbol{h}, \boldsymbol{y}) = \left(\ \{h_1 - h_2\,T\}_T \ \middle|\ \{\partial_T y_2(T)\}_T \ \middle|\ \left\{\tfrac{1}{2}\,\partial_T y_1(T)\right\}_T\ \right).$$

The first variation of the strain energy (4.2) is calculated as

$$\begin{array}{rcl} \delta W & = & \dfrac{\mathrm{d}W}{\mathrm{d}\boldsymbol{E}}(\tilde{\boldsymbol{E}}_{\boldsymbol{h}}) \cdot \delta\boldsymbol{E} = \displaystyle\int_{-a+2}^{+a/2} \left(\ * \ \middle|\ \lambda\,E_1 + (2\,\mu + \lambda)\,E_2 \ \middle|\ 4\,\mu\,E_3\ \right) \cdot \delta\boldsymbol{E}(T)\,\mathrm{d}T \\ & = & \displaystyle\int_{-a+2}^{+a/2} \left(\ * \ \middle|\ \lambda\,(h_1 - h_2\,T) + (2\,\mu + \lambda)\,\partial_T y_2 \ \middle|\ 2\,\mu\,\partial_T y_1\ \right) \cdot \delta\boldsymbol{E}(T)\,\mathrm{d}T, \end{array}$$

where again stars denote values that play no role in the following.

By setting the variation of strain as $\delta\boldsymbol{E} = \frac{\partial \tilde{\boldsymbol{E}}(\boldsymbol{h},\boldsymbol{y})}{\partial \boldsymbol{y}} \cdot \hat{\boldsymbol{y}} = \left(\ \{0\}_T \ \middle| \ \{\partial_T \hat{y}_2\}_T \ \middle| \ \left\{\frac{1}{2}\,\partial_T \hat{y}_1\right\}_T \ \right)$ as in equation (2.6), we obtain the principle of virtual work as

$$\forall(\hat{y}_1,\hat{y}_2) \quad \int_{-a/2}^{+a/2} \left(-(2\,\mu\,\partial_T y_1)\,\frac{1}{2}\,\partial_T \hat{y}_1 + f_1^{\boldsymbol{h}}\,\hat{y}_1\right) \mathrm{d}T + \int_{-a/2}^{+a/2} (-(\lambda\,(h_1 - h_2\,T) + (2\,\mu+\lambda)\,\partial_T y_2)\,\partial_T \hat{y}_2 + f_2^{\boldsymbol{h}}\,\hat{y}_2)\,\mathrm{d}T = 0$$

where $\boldsymbol{f}^{\boldsymbol{h}} = (f_1^{\boldsymbol{h}}, f_2^{\boldsymbol{h}})$ is a Lagrange multiplier.

The solution satisfying the constraint $\boldsymbol{q}(\boldsymbol{y}) = \boldsymbol{0}$ is found as

$$\begin{array}{rcl} y_1^{\boldsymbol{h}} & = & \{0\}_T \\ y_2^{\boldsymbol{h}} & = & \left\{-\nu\,h_1\,T + \nu\,h_2\,\left(\frac{T^2}{2} - \frac{a^2}{24}\right)\right\}_T \\ \boldsymbol{f}^{\boldsymbol{h}} & = & \boldsymbol{0} \end{array}$$

where we have defined the 2-d Poisson's ratio $\nu = \frac{\lambda}{2\,\mu+\lambda}$. We also define the Young's modulus in 2d as $Y = \frac{4\,\mu\,(\lambda+\mu)}{2\,\mu+\lambda}$ (note that these expressions of ν and Y are valid for 2d elasticity but not for 3d elasticity).

We can then calculate the quantities characterizing the homogeneous solutions from equation (3.2) as

$$\begin{array}{rcl} \boldsymbol{E}_{\boldsymbol{h}} & = & \left(\ \{h_1 - h_2\,T\}_T \ \middle| \ \{-\nu\,(h_1 - \,h_2\,T)\}_T \ \middle| \ \{0\}_T \ \right) \\ W_{\mathrm{hom}}(\boldsymbol{h}) & = & \frac{1}{2}\,(Y\,a\,h_1^2 + Y\,I\,h_2^2) \\ \boldsymbol{\Sigma}_{\boldsymbol{h}} \cdot \delta\boldsymbol{E} & = & \int_{-a+2}^{+a/2} \left(\ Y\,(h_1 - h_2\,T) \ \middle| \ 0 \ \middle| \ 0 \ \right) \cdot \delta\boldsymbol{E}(T)\,\mathrm{d}T \\ \delta\boldsymbol{E} \cdot \boldsymbol{K}_{\boldsymbol{h}} \cdot \delta\boldsymbol{E} & = & \int_{-a+2}^{+a/2} \delta\boldsymbol{E}(T) \cdot \begin{pmatrix} * & * & 0 \\ * & 2\,\mu+\lambda & 0 \\ 0 & 0 & 4\,\mu \end{pmatrix} \cdot \delta\boldsymbol{E}(T)\,\mathrm{d}T, \end{array} \tag{4.5}$$

where $I = \int_{-a/2}^{+a/2} T^2\,\mathrm{d}T = \frac{a^3}{12}$ is the geometric moment of inertia of the cross-section.

4.4. Change of microscopic variable

Seeking the microscopic displacement as $\boldsymbol{y}(S) = \boldsymbol{y}_{\boldsymbol{h}}(S) + \boldsymbol{z}(S)$ from equation (2.8), we can calculate the strain in terms of the new microscopic variable $\boldsymbol{z}$ as

$$\boldsymbol{e}_{\boldsymbol{h}}(\boldsymbol{h}^\dagger, \boldsymbol{h}^\ddagger; \boldsymbol{z}, \boldsymbol{z}^\dagger, \boldsymbol{z}^\ddagger) = \Big(\ \{h_1 + z_1^\dagger(T) - h_2\,T\}_T \ \Big| \ \{-\nu\,(h_1 - h_2\,T) + \partial_T\,z_2\}_T \ \Big| \ \ldots \\ \Big| \ \left\{\frac{1}{2}\,\left(-\nu\,h_1^\dagger\,T + \nu\,h_2^\dagger\left(\frac{T^2}{2} - \frac{a^2}{24}\right) + \partial_T z_1 + z_2^\dagger\right)\right\}_T \ \Big).$$

where $\boldsymbol{h} = (h_1, h_2)$, $\boldsymbol{h}^\dagger = (h_1^\dagger, h_2^\dagger)$, $\boldsymbol{z} = (\{z_1(T)\}_T, \{z_2(T)\}_T)$ and $\boldsymbol{z}^\dagger = (\{z_1^\dagger(T)\}_T, \{z_2^\dagger(T)\}_T)$. For the linear elastic block, the structure coefficients do not depend on $\boldsymbol{h}^\ddagger$ or $\boldsymbol{z}^\ddagger$.

The structure coefficients introduced in equation (2.11) are then obtained as

$$\boldsymbol{e}_{000}^{10}(\boldsymbol{h}) \cdot \boldsymbol{h}^\dagger = \left(\ \boldsymbol{0} \ \middle| \ \boldsymbol{0} \ \middle| \ \left\{-\frac{\nu}{2}\,\left(h_1^\dagger\,T - \,h_2^\dagger\left(\frac{T^2}{2} - \frac{a^2}{24}\right)\right)\right\}_T \ \right)$$

$$\boldsymbol{e}_{000}^{20}(\boldsymbol{h}) = \boldsymbol{0} \quad \boldsymbol{e}_{000}^{01}(\boldsymbol{h}) = \boldsymbol{0} \quad \boldsymbol{h}^\dagger \cdot \boldsymbol{e}_{100}^{10}(\boldsymbol{h}) \cdot \boldsymbol{z} = \boldsymbol{0} \quad \boldsymbol{e}_{100}^{00}(\boldsymbol{h}) \cdot \boldsymbol{z} = \left(\ \boldsymbol{0} \ \middle| \ \{\partial_T\,z_2\}_T \ \middle| \ \left\{\frac{1}{2}\,\partial_T z_1\right\}_T \ \right)$$

$$\boldsymbol{z} \cdot \boldsymbol{e}_{200}^{00}(\boldsymbol{h}) \cdot \boldsymbol{z} = \boldsymbol{0} \quad \boldsymbol{e}_{010}^{00}(\boldsymbol{h}) \cdot \boldsymbol{z}^\dagger = \left(\ \{z_1^\dagger\}_T \ \middle| \ \boldsymbol{0} \ \middle| \ \left\{\frac{1}{2}\,z_2^\dagger\right\}_T \ \right).$$

Next, the operators introduced in (2.12) are calculated as follows,

$$\begin{array}{rcl} \boldsymbol{A}_{\boldsymbol{h}} & = & \boldsymbol{0} \\ \boldsymbol{C}_{\boldsymbol{h}}^{(0)} & = & \boldsymbol{0} \\ \boldsymbol{C}_{\boldsymbol{h}}^{(1)} \cdot \boldsymbol{z} & = & \int_{-a+2}^{+a/2} Y\,(h_1 - h_2\,T)\,z_1\,\mathrm{d}T \\ \frac{1}{2}\,\boldsymbol{h}^\dagger \cdot \boldsymbol{B}_{\boldsymbol{h}}^{(0)} \cdot \boldsymbol{h}^\dagger & = & \frac{1}{2}\,\int_{-a+2}^{+a/2} \mu\,\nu^2\,\left(h_1^\dagger\,T - \frac{h_2^\dagger}{2}\left(T^2 - \frac{a^2}{12}\right)\right)^2 \mathrm{d}T \\ & = & \frac{1}{2}\,\mu\,\nu^2\,\left(\frac{a^3}{12}\,{h_1^\dagger}^2 + \frac{a^5}{720}\,{h_2^\dagger}^2\right) \\ \boldsymbol{h}^\dagger \cdot \boldsymbol{B}_{\boldsymbol{h}}^{(1)} \cdot \boldsymbol{z} & = & -\nu\,\mu\,\int_{-a+2}^{+a/2} \left(h_1^\dagger\,T - \frac{h_2^\dagger}{2}\,\left(T^2 - \frac{a^2}{12}\right)\right)\,\partial_T z_1\,\mathrm{d}T - Y\,\int_{-a+2}^{+a/2} (h_1^\dagger - h_2^\dagger\,T)\,z_1\,\mathrm{d}T \\ \frac{1}{2}\,\boldsymbol{z} \cdot \boldsymbol{B}_{\boldsymbol{h}}^{(2)} \cdot \boldsymbol{z} & = & \frac{1}{2}\,\int_{-a+2}^{+a/2} (2\,\mu+\lambda)\,(\partial_T\,z_2)^2 + \mu\,(\partial_T z_1)^2\,\mathrm{d}T. \end{array} \tag{4.6}$$

4.5. Local optimization problem

The correction $\boldsymbol{z}_{\rm opt} = \left(z_1^{\rm opt}, z_2^{\rm opt}\right)$ to the cross-sectional displacement is found by writing down the variational problem (2.14),

$$\forall(\hat{z}_1(T), \hat{z}_2(T)) \quad \int_{-a+2}^{+a/2} \left[\mu\left(\partial_T z_1^{[1]} - \nu\left(-h_2'\,\frac{T^2}{2} + h_1'\,T + h_2'\,\frac{a^2}{24}\right)\right)\partial_T \hat{z}_1 - Y\,(h_1' - h_2'\,T)\,\hat{z}_1\right]\,{\rm d}T \ldots$$
$$+ \int_{-a+2}^{+a/2} \left[(2\,\mu+\lambda)\,\partial_T\, z_2^{\rm opt}\,\partial_T\,\hat{z}_2\right]\,{\rm d}T - \frac{1}{a}\int_{-a/2}^{+a/2}\left(f_1^{\rm opt}\,\hat{z}_1 + f_2^{\rm opt}\,\hat{z}_2\right)\,{\rm d}T = 0.$$

We proceed to solve this variational problem together with the incremental constraint $\left\langle z_1^{\rm opt}\right\rangle = \left\langle z_2^{\rm opt}\right\rangle = 0$. As there is no source term in factor of $\hat{z}_2$, the transverse solution is easily found as $z_2^{\rm opt}(T) = 0$ and $f_2^{\rm opt} = 0$.

The remaining terms in the variational problem above concern the axial correction, and can be rearranged as

$$\forall\hat{z}_1(T) \quad \int_{-a+2}^{+a/2}\left(\left(\frac{f_1^{\rm opt}}{a} + Y\,h_1'\right) - Y\,h_2'\,T\right)\hat{z}_1 - \mu\left(\partial_T z_1^{\rm opt} - \nu\left(-h_2'\,\frac{T^2}{2} + h_1'\,T + h_2'\,\frac{a^2}{24}\right)\right)\partial_T\hat{z}_1\,{\rm d}T = 0.$$

The solution to this equation satisfying the constraint $\left\langle z_1^{\rm opt}\right\rangle = 0$ can be worked out as

$$\begin{array}{rcl} f_1^{\rm opt} & = & -a\,h_1'\,Y \\ z_1^{\rm opt}(T) & = & \frac{h_1'\,\nu}{2}\left(T^2 - \frac{a^2}{12}\right) - \frac{h_2'}{24}\left((6+5\,\nu)\,a^2\,T - 4\,(2+\nu)\,T^3\right). \end{array}$$

The detailed expression of $z_1^{\rm opt}$ will not be used, other than to evaluate the following integral,

$$\int_{-a/2}^{a/2}\left(\partial_T z_1^{\rm opt}\right)^2\,{\rm d}T = \frac{a^3\,\nu^2}{12}\,{h_1'}^2 + \left(\frac{1}{30} + \frac{11\,\nu}{180} + \frac{7\,\nu^2}{240}\right)a^5\,{h_2'}^2.$$

To sum up, the displacement correction $\boldsymbol{z}_{\rm opt} = \left(z_1^{\rm opt}, z_2^{\rm opt}\right)$ can be written in terms of a fixed basis of functions as $\boldsymbol{z}_{\rm opt} = \boldsymbol{Z}^{\boldsymbol{h}}_{\rm opt}\cdot\boldsymbol{h}'$, where

$$\boldsymbol{Z}^{\boldsymbol{h}}_{\rm opt} = \begin{pmatrix} \frac{\nu}{2}\left(T^2 - \frac{a^2}{12}\right) & -\frac{1}{24}\left((6+5\,\nu)\,a^2\,T - 4\,(2+\nu)\,T^3\right) \\ 0 & 0 \end{pmatrix}.$$

The entries in the top-left (respectively top-right) slot is a longitudinal displacement along $\boldsymbol{e}_x$ in response to a gradient of axial strain $h_1 = U'$ (respectively, to a gradient of curvature $h_2 = V''$).

The necessary stability condition from section 2.7 requires $2\,\mu + \lambda \geq 0$ and $\mu \geq 0$, which are standard condition of material stability in 2d, as discussed for example in Barenblatt and Joseph (1997).

4.6. Regularized model

Two last operators are defined in equation(2.17). They can now be evaluated as

$$\boldsymbol{h}^\dagger\cdot\boldsymbol{B}_{\boldsymbol{h}}\cdot\boldsymbol{h}^\dagger = \mu\,\nu^2\left(\frac{a^3}{12}\,{h_1^\dagger}^2 + \frac{a^5}{720}\,{h_2^\dagger}^2\right) - \mu\int_{-a+2}^{+a/2}(\partial_T z_1)^2\,{\rm d}T$$
$$= -\mu\,a^5\left(\frac{1}{30} + \frac{11\,\nu}{180} + \frac{\nu^2}{36}\right){h_2^\dagger}^2 = -Y\,a^5\,\frac{6+5\,\nu}{360}\,{h_2^\dagger}^2 \quad (4.7)$$

and

$$\boldsymbol{C}_{\boldsymbol{h}}\cdot\boldsymbol{h}^\dagger = \int_{-a+2}^{+a/2} Y\,(h_1 - h_2\,T)\begin{pmatrix} \frac{\nu}{2}\left(T^2 - \frac{a^2}{12}\right) \\ -\frac{1}{24}\left((6+5\,\nu)\,a^2\,T - 4\,(2+\nu)\,T^3\right)\end{pmatrix}\cdot\boldsymbol{h}^\dagger\,{\rm d}T = Y\,a^5\,\frac{12+11\,\nu}{720}\,h_2\,h_2^\dagger.$$

In addition, recall that $\boldsymbol{A_h} = \boldsymbol{0}$.

Using equation (2.16), we obtain the energy function of the 1d model as

$$\Phi^\star[\boldsymbol{h}] = \int_0^L \frac{1}{2}\,(Y\,a\,h_1^2 + Y\,I\,h_2^2)\,\mathrm{d}S + Y\,a^5\,\frac{12+11\,\nu}{720}\,[h_2\,h_2']_0^L - \frac{1}{2}\,Y\,a^5\,\frac{6+5\,\nu}{360}\int_0^L h_2'^2\,\mathrm{d}S, \tag{4.8}$$

where $h_1 = U'$ denotes the axial stretch and $h_2 = V''$ denotes the curvature.

4.7. Comments

We have recovered the classical Euler-Bernoulli rod model at the dominant order, with a stretching modulus $Y\,a$ and a bending modulus $Y\,I$. Indeed, the first step of the reduction method yields classical structural model (i.e., without the gradient effect), see the expression of W_{hom} in equation (4.5).

As the operator $\frac{1}{2}\,\boldsymbol{z}\cdot\boldsymbol{B}_{\boldsymbol{h}}^{(2)}\cdot\boldsymbol{z}$ in equation (4.6) is non-negative, the necessary condition of stability with respect to the microscopic degrees of freedom is satisfied, see §2.7. However, the coefficient of the gradient term $h_2'^2$ in (4.8) is negative, like the second-gradient modulus $\boldsymbol{B_h}$ acting on the macroscopic degrees of freedom, see (4.7). As a result, $\Phi^\star[\boldsymbol{h}]$ can be decreased without bound by means of small-scale oscillations. This behavior can likely be regularized by pushing the expansion to a higher order. In its present form, the functional (4.8) should not be used to set up a minimization or to analyze stability; it is still useful, as its stationary points provide a more accurate approximation of the 3d solution than that of the Euler-Bernoulli model.

To connect with the existing literature, we have worked out this example in the limited context of linear elasticity but the derivation can be extended easily to deal, e.g., with a nonlinear constitutive law, a nonlinear geometry, as demonstrated in the following section. While previous work has been focused on deriving order by order solutions to the 3d equilibrium equations, our relaxation method makes use of the variational structure of these equations by working directly on the energy. This, together with the fact that the hard work underlying the derivation of the general method in section 2 and Appendix A has been done once for all, simplifies the reduction of any particular structural model considerably.

The only gradient effect present in equation (4.8) comes from the gradient of bending. The absence of a gradient term for stretching is a peculiarity of the linear elasticity model which we started from: a gradient effect involving the axial strain h_1 is restored if we start instead from a finite-elasticity theory, as the next example will show. In fact, it does not make much sense to derive a *higher-order rod model*, which aims at identifying subdominant corrections to the elastic energy, starting from a *linear elasticity model*: the linearization underlying the linear elasticity theory suppresses subdominant contributions to the strain energy *a priori*. This fact has not been well appreciated, as most of the earlier work on higher-order beam models has been done in the framework of linear elasticity.

5. Application to a hyperelastic cylinder in tension

In our third example, we address the axisymmetric deformation of a hyperelastic cylinder. This problem is motivated by the necking of bars, a situation where deformations become localized. Necking typically involves plasticity but it can be analyzed using an equivalent elastic constitutive law obtained by the J_2 deformation theory, as long as the loading is proportional and monotonous: the equivalent hyperelastic law is such that the curve for homogeneous traction displays a maximum of the force as a function of the stretch, leading to localization. This section derives the 1d model obtained by Audoly and Hutchinson (2016) using a dedicated expansion method, this time using the general method of section 2. This worked example combines a continuous cross-section, a nonlinear elastic model, and kinematic constraints.

5.1. Finite-strain elasticity model for an axisymmetric bar

In its reference configuration, the bar is a cylinder with length L and radius ρ, and we denote by S, T and Θ the axial, radial and azimuthal coordinates, respectively, with $0 \le S \le L$, $0 \le T \le \rho$, $0 \le \Theta \le 2\,\pi$. We consider a transversely isotropic material whose elastic properties are functions of T but not of Θ or

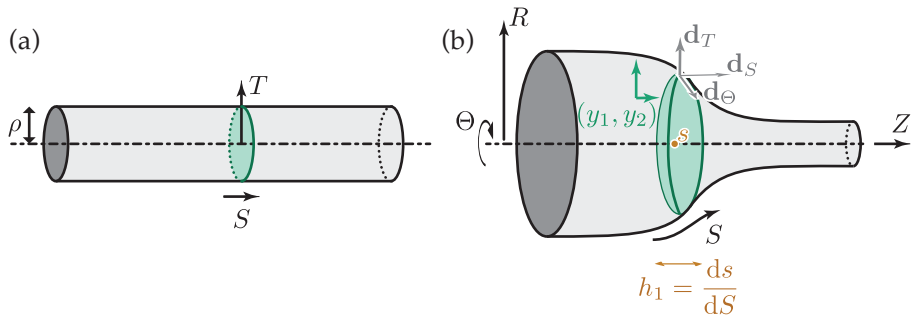

Figure 6: A nonlinearly elastic cylinder in (a) reference configuration and (b) current configuration.

S (isotropy is a particular case of transverse isotropy, so this includes homogeneous isotropic materials): this warrants that axisymmetric solutions possessing cylindrical invariance exist when the bar is subject to traction. In fact, we restrict attention to axisymmetric solutions, ignoring the possibility of localized modes involving shear bands (Triantafyllidis et al., 2007).

The coordinates (S, T) are used as Lagrangian coordinates, and we denote by $\boldsymbol{x}(S,T) = (Z(S,T), R(S,T))$ the axial and radial cylindrical coordinates of a material point initially located as (S,T), see figure 6(b). In 3d space, the final position is $Z(S,T)\,\boldsymbol{d}_S(\Theta) + R(S,T)\,\boldsymbol{d}_T$, where $(\boldsymbol{d}_S(\Theta), \boldsymbol{d}_T, \boldsymbol{d}_\Theta(\Theta))$ is the local cylindrical basis, as sketched in the figure. Denoting partial derivatives using commas in subscript, the deformation gradient is $\boldsymbol{F} = Z_{,S}\,\boldsymbol{d}_S \otimes \boldsymbol{d}_S + Z_{,T}\,\boldsymbol{d}_S \otimes \boldsymbol{d}_T + R_{,S}\,\boldsymbol{d}_T \otimes \boldsymbol{d}_S + R_{,T}\,\boldsymbol{d}_T \otimes \boldsymbol{d}_T + \frac{R}{T}\,\boldsymbol{d}_\Theta \otimes \boldsymbol{d}_\Theta$, and the strain writes $\boldsymbol{E} = \left(\ E_1 \ \middle|\ E_2 \ \middle|\ E_3 \ \middle|\ E_4\ \right)$ where

$$\begin{array}{rcl} E_1 &=& \frac{1}{2}\,(Z_{,S}^2 + R_{,S}^2 - 1) \\ E_2 &=& \frac{1}{2}\,(Z_{,T}^2 + R_{,T}^2 - 1) \\ E_3 &=& \frac{1}{2}\,(Z_{,S}\,Z_{,T} + R_{,S}\,R_{,T}) \\ E_4 &=& \frac{1}{2}\,\left(\left(\frac{R}{T}\right)^2 - 1\right). \end{array} \tag{5.1}$$

Here, $\left(\ E_1 \ \middle|\ E_2 \ \middle|\ E_3 \ \middle|\ E_4\ \right) = \left(\ \overline{E}_{SS} \ \middle|\ \overline{E}_{TT} \ \middle|\ \overline{E}_{ST} \ \middle|\ \overline{E}_{\Theta\Theta}\ \right)$ are the components of the Green–St-Venant strain $\overline{\boldsymbol{E}} = \frac{1}{2}\,(\boldsymbol{F}^T \cdot \boldsymbol{F} - \boldsymbol{I})$ from finite-elasticity theory (symbols bearing a bar on top are relevant to the full model) and $\boldsymbol{I}$ is the identity matrix.

For a transversely isotropic material, the strain energy of the bar per unit length can be written in the form

$$W(\boldsymbol{E}) = \int_0^\rho \overline{W}(E_1(S), E_3^2(S), E_2(S) + E_4(S), E_2^2(S) + E_4^2(S), E_2(S)\,E_3^2(S))\,2\,\pi\,T\,\mathrm{d}T, \tag{5.2}$$

where $\overline{W}(\overline{E}_{SS}, \overline{E}_{ST}^2, \overline{E}_{TT} + \overline{E}_{\Theta\Theta}, \overline{E}_{TT}^2 + \overline{E}_{\Theta\Theta}^2, \overline{E}_{TT}\,\overline{E}_{ST}^2)$ is the elastic potential of the material model, written in terms of a set of invariants relevant to the transverse isotropic symmetry.

5.2. Macroscopic and microscopic variables

Let us consider the coordinate $s(S)$ of the center of mass of the deformed cross-section, i.e.,

$$s(S) = \langle Z \rangle(S), \tag{5.3}$$

where $\langle f \rangle = \frac{1}{\pi\,\rho^2}\int_0^\rho f(T)\,2\,\pi\,T\,\mathrm{d}T$ denotes the average of a quantity over the cross-section. This $s(S)$ is denoted by the orange dot in figure 6(b); it does not correspond to any material point. We use a single macroscopic strain variable, defined as the apparent axial stretch

$$\boldsymbol{h}(S) = (h_1(S)) = \left(\frac{\mathrm{d}s}{\mathrm{d}S}(S)\right).$$

We use as microscopic degrees of freedom $\boldsymbol{y}$ the position of the current relative to the center of mass of the cross-section,

$$\boldsymbol{y} = (\{y_1\}_T, \{y_2\}_T),$$

such that the position in deformed configuration can be reconstructed as

$$\boldsymbol{x}(S,T) = (Z(S,T), R(S,T)) = (s(S) + y_1(S,T), y_2(S,T)).$$

In view of equation (5.3), one must enforce the kinematic constraint $\boldsymbol{q}(\boldsymbol{y}(S)) = 0$ for all S, where

$$\boldsymbol{q}(\boldsymbol{y}) = \left(\int_0^\rho y_1(T)\, 2\,\pi\, T \,\mathrm{d}T \right).$$

In terms of the macroscopic strain and microscopic displacement, the map of strain over a cross section writes, from equation (5.1),

$$\boldsymbol{E}(\boldsymbol{h}, \boldsymbol{h}^\dagger; \boldsymbol{y}, \boldsymbol{y}^\dagger, \boldsymbol{y}^\ddagger) = \begin{pmatrix} \left\{ \frac{1}{2} \left((h_1 + y_1^\dagger)^2 + (y_2^\dagger)^2 - 1 \right) \right\}_T \\ \left\{ \frac{1}{2} \left((\partial_T y_1)^2 + (\partial_T y_2)^2 - 1 \right) \right\}_T \\ \left\{ \frac{1}{2} \left((h_1 + y_1^\dagger)\, \partial_T y_1 + y_2^\dagger\, \partial_T y_2 \right) \right\}_T \\ \left\{ \frac{1}{2} \left(\left(\frac{y_2}{T} \right)^2 - 1 \right) \right\}_T \end{pmatrix}. \tag{5.4}$$

As earlier with the elastic block, and as implied by the $\{\ldots\}_T$ notation, each component of $\boldsymbol{E}(S)$ is a function defined over the cross-section.

5.3. Homogeneous solutions

A detailed analysis of homogeneous solutions is done in Appendix B.1. The main results are summarized as follows.

At the microscopic level, the cross-sections remains planar and undergo a uniform dilation with a stretch ratio $\mu_{(h_1)}$ depending on the (uniform) longitudinal stretch h_1, i.e., the microscopic displacement is of the form

$$y_1^{(h_1)} = \{0\}_T \qquad y_2^{(h_1)} = \{\mu_{(h_1)}\, T\}_T.$$

Due to the material symmetry, the microscopic stress is equi-biaxial, with a longitudinal stress $\overline{\Sigma}_\parallel(h_1, \mu_{(h_1)}) = \overline{\Sigma}_{SS}$ and a transverse stress $\overline{\Sigma}_\perp(h_1, \mu_{(h_1)}) = \overline{\Sigma}_{TT} = \overline{\Sigma}_{\Theta\Theta}$ given in terms of the elastic constitutive model by

$$\begin{array}{rcl} \overline{\Sigma}_\parallel(h_1, \mu) & = & \partial_1 \overline{W} \left(\frac{1}{2}(h_1^2 - 1), 0, \mu^2 - 1, \frac{1}{2}(\mu^2 - 1)^2, 0 \right) \\ \overline{\Sigma}_\perp(h_1, \mu) & = & \partial_3 \overline{W} \left(\frac{1}{2}(h_1^2 - 1), 0, \mu^2 - 1, \frac{1}{2}(\mu^2 - 1)^2, 0 \right) + (\mu^2 - 1)\, \partial_4 \overline{W} \left(\frac{1}{2}(h_1^2 - 1), 0, \mu^2 - 1, \frac{1}{2}(\mu^2 - 1)^2, 0 \right). \end{array} \tag{5.5}$$

Here, $\partial_i \overline{W}$ denotes the partial derivative of the strain energy with respect to the ith argument.

The equilibrium of the lateral boundary yields an implicit equation for the transverse stretch $\mu_{(h_1)}$ in terms of the longitudinal stretch,

$$\overline{\Sigma}_\perp(h_1, \mu_{(h_1)}) = 0. \tag{5.6}$$

The homogeneous microscopic strain, strain energy density, microscopic stress and tangent elastic stiffness are then given by equation (2.7) as

$$\begin{array}{rcl} \boldsymbol{E}_{\boldsymbol{h}} & = & \left(\left\{ \frac{1}{2}(h_1^2 - 1) \right\}_T \,\middle|\, \left\{ \frac{1}{2}(\mu_{(h_1)}^2 - 1) \right\}_T \,\middle|\, \{0\}_T \,\middle|\, \left\{ \frac{1}{2}(\mu_{(h_1)}^2 - 1) \right\}_T \right) \\ W_{\mathrm{hom}}(\boldsymbol{h}) & = & \int_0^\rho \overline{W} \left(\frac{1}{2}(h_1^2 - 1), 0, \mu_{(h_1)}^2 - 1, \frac{1}{2}(\mu_{(h_1)}^2 - 1)^2, 0 \right) 2\,\pi\, T \,\mathrm{d}T \\ \boldsymbol{\Sigma}_{\boldsymbol{h}} \cdot \delta\boldsymbol{E} & = & \int_0^\rho \overline{\Sigma}_\parallel(h_1, \mu_{(h_1)})\, \delta E_1(T)\, 2\,\pi\, T \,\mathrm{d}T \\ \delta\boldsymbol{E} \cdot \boldsymbol{K}_{\boldsymbol{h}} \cdot \delta\boldsymbol{E} & = & \int_0^\rho \left[4\, \overline{K}_{ST}^{ST} (\delta E_3(T))^2 + \begin{pmatrix} \delta E_1(T) \\ \delta E_2(T) \\ \delta E_4(T) \end{pmatrix} \cdot \begin{pmatrix} * & * & * \\ * & \overline{K}_{TT}^{TT} & \overline{K}_{TT}^{\Theta\Theta} \\ * & \overline{K}_{TT}^{\Theta\Theta} & \overline{K}_{TT}^{TT} \end{pmatrix} \cdot \begin{pmatrix} \delta E_1(T) \\ \delta E_2(T) \\ \delta E_4(T) \end{pmatrix} \right] 2\,\pi\, T \,\mathrm{d}T \end{array}$$

where the incremental shearing modulus reads

$$\overline{K}^{ST}_{ST} = \frac{1}{4}\,(2\,\partial_2\overline{W} + (\mu^2_{(h_1)} - 1)\,\partial_5\overline{W}). \tag{5.7}$$

In the right-hand side, the derivatives of the elastic potential $\overline{W}$ must be evaluated in the homogeneous solution $(\overline{E}_{SS}, \overline{E}^2_{ST}, \overline{E}_{TT} + \overline{E}_{\Theta\Theta}, \overline{E}^2_{TT} + \overline{E}^2_{\Theta\Theta}, \overline{E}_{TT}\,\overline{E}^2_{ST}) = \big(\frac{1}{2}\,(h_1^2 - 1), 0, \mu^2 - 1, \frac{1}{2}\,(\mu^2 - 1)^2, 0\big)$, as in equation (5.5). The expressions of the other elastic moduli do not play any role in the 1d model.

The symmetry of the material and of the homogeneous solution accounts for the particular form of the tangent moduli found above. For instance, the tangent modulus $\overline{K}^{TT}_{TT}$ in factor of $(\delta E_4)^2 = (\delta E_{\Theta\Theta})^2$ in the second variation of the elastic potential $\delta\boldsymbol{E}\cdot\boldsymbol{K_h}\cdot\delta\boldsymbol{E}$ is identical to that in factor of $(\delta E_2)^2 = (\delta E_{TT})^2$ due to the transverse isotropy, i.e., $\overline{K}^{\Theta\Theta}_{\Theta\Theta} = \overline{K}^{TT}_{TT}$.

5.4. Structure coefficients, local optimization problem

Using the homogeneous solution just obtained and the expression of the strain $\boldsymbol{E}$ in equation (5.4), one can calculate the structure coefficients relevant to the nonlinear cylinder as (details can be found in Appendix B.2)

$$\begin{array}{l}
\boldsymbol{e}^{10}_{000}(\boldsymbol{h})\cdot\boldsymbol{h}^\dagger = \Big(\ \mathbf{0}\ \Big|\ \mathbf{0}\ \Big|\ \Big\{\frac{\mu_{(h_1)}\,\nabla\mu_{(h_1)}}{2}\,T\,h_1^\dagger\Big\}_T\ \Big|\ \mathbf{0}\ \Big)\\
\boldsymbol{h}^\dagger\cdot\boldsymbol{e}^{20}_{000}(\boldsymbol{h})\cdot\boldsymbol{h}^\dagger = \big(\ \{(\nabla\mu_{(h_1)})^2\,T^2\,(h_1^\dagger)^2\}_T\ \big|\ \mathbf{0}\ \big|\ \mathbf{0}\ \big|\ \mathbf{0}\ \big)\\
\boldsymbol{e}^{01}_{000}(\boldsymbol{h}) = \mathbf{0}\quad \boldsymbol{h}^\dagger\cdot\boldsymbol{e}^{10}_{100}(\boldsymbol{h})\cdot(z_1,z_2) = \big(\ \mathbf{0}\ \big|\ \mathbf{0}\ \big|\ *\ \big|\ \mathbf{0}\ \big)\\
\boldsymbol{e}^{00}_{100}(\boldsymbol{h})\cdot(z_1,z_2) = \Big(\ \mathbf{0}\ \Big|\ \{\mu_{(h_1)}\,\partial_T z_2(T)\}_T\ \Big|\ \big\{\tfrac{h_1}{2}\,\partial_T z_1(T)\big\}_T\ \Big|\ \Big\{\mu_{(h_1)}\,\frac{z_2(T)}{T}\Big\}_T\ \Big)\\
(z_1,z_2)\cdot\boldsymbol{e}^{00}_{200}(\boldsymbol{h})\cdot(z_1,z_2) = \Big(\ \mathbf{0}\ \Big|\ \{(\partial_T z_1(T))^2 + (\partial_T z_2(T))^2\}_T\ \Big|\ \mathbf{0}\ \Big|\ \Big\{\Big(\frac{z_2(T)}{T}\Big)^2\Big\}_T\ \Big)\\
\boldsymbol{e}^{00}_{010}(\boldsymbol{h})\cdot(z_1^\dagger,z_2^\dagger) = \big(\ \{h_1\,z_1^\dagger(T)\}_T\ \big|\ \mathbf{0}\ \big|\ *\ \big|\ \mathbf{0}\ \big)\,.
\end{array} \tag{5.8}$$

This yields the first set of operators as

$$\begin{array}{rcl}
\boldsymbol{A_h} &=& \mathbf{0}\\
\boldsymbol{C}^{(0)}_{\boldsymbol{h}} &=& \mathbf{0}\\
\boldsymbol{C}^{(1)}_{\boldsymbol{h}}\cdot\boldsymbol{z} &=& \overline{\Sigma}_\parallel(h_1,\mu_{(h_1)})\,h_1\,\int_0^\rho z_1(T)\,2\,\pi\,T\,\mathrm{d}T\\
\frac{1}{2}\,\boldsymbol{h}^\dagger\cdot\boldsymbol{B}^{(0)}_{\boldsymbol{h}}\cdot\boldsymbol{h}^\dagger &=& \frac{1}{2}\,(h_1^\dagger)^2\,\frac{2\,\pi\,\rho^4}{4}\,(\nabla\mu_{(h_1)})^2\,(\mu^2_{(h_1)}\,\overline{K}^{ST}_{ST} + \overline{\Sigma}_\parallel(h_1,\mu_{(h_1)}))\\
\boldsymbol{h}^\dagger\cdot\boldsymbol{B}^{(1)}_{\boldsymbol{h}}\cdot\boldsymbol{z} &=& h_1^\dagger\,\Big(\overline{K}^{ST}_{ST}\,\mu_{(h_1)}\,\nabla\mu_{(h_1)}\,h_1\,\int_0^\rho T\,\partial_T z_1(T)\,2\,\pi\,T\,\mathrm{d}T\Big)\\
&& -h_1^\dagger\,\frac{\mathrm{d}(\overline{\Sigma}_\parallel(h_1,\mu_{(h_1)})\,h_1)}{\mathrm{d}h_1}\,\int_0^\rho z_1(T)\,2\,\pi\,T\,\mathrm{d}T\\
\frac{1}{2}\,\boldsymbol{z}\cdot\boldsymbol{B}^{(2)}_{\boldsymbol{h}}\cdot\boldsymbol{z} &=& \frac{1}{2}\,\int_0^\rho h_1^2\,\overline{K}^{ST}_{ST}\,(\partial_T z_1(T))^2\,2\,\pi\,T\,\mathrm{d}T\\
&& +\frac{1}{2}\,\int_0^\rho \begin{pmatrix}\partial_T z_2(T)\\ \frac{z_2(T)}{T}\end{pmatrix}\cdot\boldsymbol{Q}(h_1)\cdot\begin{pmatrix}\partial_T z_2(T)\\ \frac{z_2(T)}{T}\end{pmatrix}\,2\,\pi\,T\,\mathrm{d}T
\end{array} \tag{5.9}$$

where

$$\boldsymbol{Q}(h_1) = \mu^2_{(h_1)}\,\begin{pmatrix}\overline{K}^{TT}_{TT} & \overline{K}^{\Theta\Theta}_{TT}\\ \overline{K}^{\Theta\Theta}_{TT} & \overline{K}^{TT}_{TT}\end{pmatrix}$$

and we recall that ∇ is a gradient with the respect to the macroscopic strain $\boldsymbol{h}$, i.e.,

$$\nabla\mu_{(h_1)} = \frac{\mathrm{d}\mu_{(h)}}{\mathrm{d}h}(h_1).$$

This quantity $\nabla\mu_{(h_1)}$ can be found by differentiating the implicit equation (5.6).

The local correction $\boldsymbol{z} = \boldsymbol{z}^{\rm opt}$ is obtained by making the quantity $\frac{1}{2}\,\boldsymbol{z}\cdot\boldsymbol{B}^{(2)}_{\boldsymbol{h}}\cdot\boldsymbol{z}+\boldsymbol{h}^{\dagger}\cdot\boldsymbol{B}^{(1)}_{\boldsymbol{h}}\cdot\boldsymbol{z}$ stationary for given values of $\boldsymbol{h}$ and $\boldsymbol{h}^{\dagger}$, subject to the constraint $\boldsymbol{q}(\boldsymbol{z}) = \boldsymbol{0}$. This variational problem is solved in Appendix B.3. The solution can be cast in the form $\boldsymbol{z}_{\rm opt}(S) = \boldsymbol{Z}^{\boldsymbol{h}(S)}_{\rm opt}\cdot\boldsymbol{h}'(S)$ announced in equation (2.15) with

$$\boldsymbol{Z}^{\boldsymbol{h}(S)}_{\rm opt} = \begin{pmatrix} \left\{-\frac{1}{2}\,\frac{\mu_{(h1)}\,\nabla\mu_{(h_1)}}{h_1}\,\left(T^2-\frac{\rho^2}{2}\right)\right\}_T \\ \{0\}_T \end{pmatrix}. \tag{5.10}$$

Stated differently, the corrective displacement is purely longitudinal ($z_2^{\rm opt} = 0$), and parabolic: $z_1^{\rm opt} = -\frac{1}{2}\,\frac{\mu_{(h1)}\,\nabla\mu_{(h_1)}}{h_1}\,\left(T^2-\frac{\rho^2}{2}\right)\,h_1'(S)$.

The following integral, which is required later on, can be calculated based on the expressions of $z_1^{\rm opt}$ just found as

$$\int_0^{\rho}\left(\partial_T z_1^{\rm opt}(T)\right)^2\,2\,\pi\,T\,{\rm d}T = \frac{\pi\,\rho^4}{2}\,\left(\frac{\mu_{(h_1)}\,\nabla\mu_{(h_1)}}{h_1}\right)^2\,h_1'^2. \tag{5.11}$$

A necessary condition for the stability of this microscopic solution (see §2.7) is that $\overline{K}^{ST}_{ST}\geq 0$ and the submatrix of the tangent moduli $\begin{pmatrix} \overline{K}^{\Theta\Theta}_{\Theta\Theta} & \overline{K}^{\Theta\Theta}_{TT} \\ \overline{K}^{\Theta\Theta}_{TT} & \overline{K}^{TT}_{TT}\end{pmatrix}$ is positive.

5.5. Regularized model

We can finally calculate the two operators entering in the 1d model as

$$\begin{array}{rcl} \frac{1}{2}\,\boldsymbol{h}'\cdot\boldsymbol{B}_{\boldsymbol{h}}\cdot\boldsymbol{h}^{'} & = & \frac{1}{2}\,\boldsymbol{h}'\cdot\boldsymbol{B}^{(0)}_{\boldsymbol{h}}\cdot\boldsymbol{h}^{'}-\frac{1}{2}\,\boldsymbol{z}_{\rm opt}\cdot\boldsymbol{B}^{(2)}_{\boldsymbol{h}}\cdot\boldsymbol{z}_{\rm opt} \\ & = & \frac{1}{2}\,h_1'^2\,\frac{2\,\pi\,\rho^4}{4}\,(\nabla\mu_{(h_1)})^2\,(\overline{\Sigma}_{\parallel}(h_1,\mu_{(h_1)})+\mu^2_{(h_1)}\,\overline{K}^{ST}_{ST})-\frac{1}{2}\,h_1^2\,\overline{K}^{ST}_{ST}\,\int_0^{\rho}(\partial_T z_1(T))^2\,2\,\pi\,T\,{\rm d}T \\ & = & \frac{h_1'^2}{2}\,\frac{\pi\,\rho^4}{2}\,(\nabla\mu_{(h_1)})^2\,\overline{\Sigma}_{\parallel}(h_1,\mu_{(h_1)}) \end{array}$$

where we have used the equilibrium condition (5.6) and the identity (5.11).

The operator $\boldsymbol{C}_{\boldsymbol{h}}$ reads

$$\boldsymbol{C}_{\boldsymbol{h}}\cdot\boldsymbol{h}^{'} = \boldsymbol{C}^{(0)}_{\boldsymbol{h}}\cdot\boldsymbol{h}^{'}+\boldsymbol{C}^{(1)}_{\boldsymbol{h}}\cdot\boldsymbol{z}^{\boldsymbol{h}}_{\rm opt} = \overline{\Sigma}_{\parallel}(h_1,\mu_{(h_1)})\,h_1\,\int_0^{\rho}z_1^{\rm opt}(T)\,2\,\pi\,T\,{\rm d}T = 0.$$

Switching to the more familiar notation $\lambda(S)$ for the apparent stretch $\lambda = h_1$, we finally obtain the 1d energy governing the cylinder as

$$\Phi^{\star}[\lambda] = \int_0^L W_{\rm hom}(\lambda(S))\,{\rm d}S+\frac{1}{2}\,\int_0^L B(\lambda(S))\,\lambda'^2(S)\,{\rm d}S, \tag{5.12a}$$

where $W_{\rm hom}(\lambda) = \int_0^{\rho}\overline{W}\left(\frac{1}{2}\,(\lambda^2-1),0,\mu^2_{(\lambda)}-1,\frac{1}{2}\,(\mu^2_{(\lambda)}-1)^2,0\right)\,2\,\pi\,T\,{\rm d}T$ is the energy of the homogeneous solution per unit length, the strain-gradient modulus is given by

$$B(\lambda) = \frac{\pi\,\rho^4}{2}\,\left(\frac{{\rm d}\mu_{(\lambda)}}{{\rm d}\lambda}\right)^2\,\overline{\Sigma}_{\parallel}(\lambda,\mu_{(\lambda)}), \tag{5.12b}$$

and the transverse stretch $\mu_{(\lambda)}$ is found by solving the transverse equilibrium of a homogeneous solution, $\overline{\Sigma}_{\perp}(\lambda,\mu_{(\lambda)}) = 0$.

5.6. Comments

We have recovered in equation (5.12) the energy functional derived by Audoly and Hutchinson (2016). As earlier with the membrane model, see §3, the strain-gradient modulus $B(\lambda)$ is directly proportional to the pre-stress $\overline{\Sigma}_{\|}$ of the homogeneous solution, and does not depend on the elastic moduli. This can be explained as follows. The expression of the operators $\boldsymbol{B}_{\boldsymbol{h}}^{(i)}$ in equation (2.12), reveal that the contribution to the strain-gradient modulus coming from the elastic moduli arises fully from the expansion of $\frac{1}{2}\,\boldsymbol{e}_{[1]}\cdot\boldsymbol{K}_{\boldsymbol{h}}\cdot\boldsymbol{e}_{[1]}$, where $\boldsymbol{e}_{[1]}=\boldsymbol{e}_{000}^{10}\cdot\boldsymbol{h}'+\boldsymbol{e}_{100}^{00}\cdot\boldsymbol{z}$ is the first-order correction to the strain, see also equation (A.6). If the correction $\boldsymbol{z}$ manages to cancel out entirely the strain $\boldsymbol{e}_{000}^{10}\cdot\boldsymbol{h}'$ arising from the gradient effect, then $\boldsymbol{e}_{[1]}=\boldsymbol{0}$ and the strain-gradient modulus arises from the pre-strain $\boldsymbol{\Sigma}_{\boldsymbol{h}}$ only. This is what happens with both the axisymmetric membrane, for which $\boldsymbol{e}_{000}^{10}\cdot\boldsymbol{h}'=\boldsymbol{0}$ from equation (3.3), and for the axisymmetric cylinder, for which $\boldsymbol{e}_{000}^{10}\cdot\boldsymbol{h}'$ is a shear strain that is canceled out by the out of plane deformation of the cross-section, as discussed by Audoly and Hutchinson (2016). For the bending of an elastic block, however, the corrective displacement $\boldsymbol{z}$ does not fully suppresses the first order strain, $\boldsymbol{e}_{[1]}\neq\boldsymbol{0}$, and the elastic moduli enter into the expression of the strain-gradient modulus.

6. Conclusion and discussion

We have presented a systematic reduction method which, given a structural model representing a prismatic elastic solid, yields a 1d model that captures the strain gradient effect. The method implements a two-scale expansion and is asymptotically exact. It is based on a choice of macroscopic strain variables which are retained in the 1d model, and a choice of microscopic variables which are relaxed during the reduction process. It can be applied as a simple recipe, i.e., it requires one to follow a systematic sequence of steps in order. The method retains the nonlinearity of the initial model, and can account for large and inhomogeneous changes in the shapes of cross-sections.

As illustrated by the worked examples, this method can be used to recover known 1d models for structures in a systematic and unified way. In future work, it will be used to derive original 1d models, e.g., for structures possessing highly deformable cross-sections, such as tape springs, or having large and inhomogeneous pre-stress (Liu et al., 2014; Lestringant and Audoly, 2017). The method can also be applied to the analysis of localization, which is ubiquitous in slender structures. In the absence of 1d models capturing the gradient effect, the various examples of localization have been addressed using equations that are specific to each particular structure, such as the axisymmetric membrane theory for bulges in balloons (Fu et al., 2008; Pearce and Fu, 2010); the authors have suggested recently that, by using dimension reduction, it is possible to analyze the various examples of localization in a unified mathematical framework (Lestringant and Audoly, 2018).

We close this paper with a few general remarks.

In the reduction method, the choice of the macroscopic strain $\boldsymbol{h}$ has been left to the user. This choice actually reflects how the applied load scales with the slenderness parameter (note that the external load has not appeared in our reduction reduction method). The scaling assumptions for the load are a key ingredient in dimension reduction, and different assumptions can lead to different 1d model (Marigo and Meunier, 2006). Similarly, different choices of $\boldsymbol{h}$ ultimately lead to different 1d models using our method. Consider for instance what happens if we add a 'strong' external shearing force $\boldsymbol{g}$ on the linear elastic block, $\boldsymbol{g}(S,T)=G(S)\,\frac{T}{a^3/12}\,\boldsymbol{e}_x$. This external load induces a moment $G(S)\,\boldsymbol{e}_z$ perpendicular to the plane of the block, in each cross-section. The kinematic quantity conjugate to $\boldsymbol{g}$ is the average rotation of the cross-section, which in the linear setting reads $\frac{1}{a^2/12}\langle\boldsymbol{y}\cdot(T\,\boldsymbol{e}_x)\rangle=\frac{\langle T\,u\rangle}{a^2/12}+V'$. This external load can therefore be handled by including an additional kinematic constraint $\langle T\,u\rangle(S)=\varphi(S)$ in the reduction method, and by augmenting macroscopic strain $\boldsymbol{h}$ with this new internal variable, $h_3=\varphi$. The reduction method has to be redone, yielding this time a Timoshenko beam model. The external load is then taken into account simply by coupling the load intensity $G(S)$ with $\frac{\varphi(S)}{a^2/12}+V'(S)$. Note that this modification of the reduction procedure is required if, and only if, the external load is strong and inhomogeneous enough that it modifies significantly the natural microscopic displacement. For mild applied force, the external moment $G(S)$ can be coupled directly to the macroscopic rotation V', saving one from the need to amend the dimension reduction.

In their analysis of a 1d model for stretched bars, Coleman and Newman (1988) have proposed a derivation of the gradient effect starting from the assumption that the kinematics of the classical bar model without gradient effect remains valid, i.e., that the cross-sections remain planar. A similar approximation has been used by several authors in various derivations of strain gradient models. In our notation, this amounts to neglecting the microscopic correction $\boldsymbol{z}$ arising from the gradient effect, i.e., to set $\boldsymbol{Z}_{\rm opt}^{\boldsymbol{h}(S)} = \boldsymbol{0}$, see equation (2.15). Equation (2.17) then yields $\boldsymbol{B}_{\boldsymbol{h}} = \boldsymbol{B}_{\boldsymbol{h}}^{(0)}$. The inequality (2.7) shows that the strain gradient modulus derived from this kinematic assumption has a larger strain-gradient elastic modulus $\boldsymbol{B}_{\boldsymbol{h}}^{(0)}$ than the true modulus predicted by our method with due account for the microscopic relaxation $\boldsymbol{z}$, as noted by Audoly and Hutchinson (2016). This is not surprising, as our approach relaxes the strain energy optimally by design, while the former does not.

For the sake of simplicity, we have assumed that the full model is invariant along the longitudinal direction. It is quite simple to extend the method to the case where the geometry and/or elastic properties of the full model vary slowly in the longitudinal direction, i.e., depend on the stretched variable $\tilde{S}$ used in Appendix A. An additional explicit dependence on $\tilde{S}$ must then be added to the various quantities entering into the analysis, such as W, $\boldsymbol{E}_{\boldsymbol{h}}$, $W_{\rm hom}$, $\boldsymbol{\Sigma}_{\boldsymbol{h}}$, etc. This brings in a single significant change: in the integrand of $\tilde{\Phi}_{[2]}$ in equation (A.8), one needs to include two extra terms $-\left[\frac{{\rm d}\boldsymbol{C}_{\boldsymbol{h}}^{(0)}}{{\rm d}\tilde{S}}(\tilde{S})\right]_{\boldsymbol{h}=\boldsymbol{h}(\tilde{S})}\cdot\dot{\boldsymbol{h}}$ and $-\left[\frac{{\rm d}\boldsymbol{C}_{\boldsymbol{h}}^{(1)}}{{\rm d}\tilde{S}}(\tilde{S})\right]_{\boldsymbol{h}=\boldsymbol{h}(\tilde{S})}\cdot\boldsymbol{z}_{[1]}$ in order to cancel out the extra terms coming from the expansion of the *total* derivatives $\frac{{\rm d}(\boldsymbol{C}_{\boldsymbol{h}(\tilde{S})}^{(0)}(\tilde{S}))}{{\rm d}\tilde{S}}\cdot\dot{\boldsymbol{h}}+\frac{{\rm d}(\boldsymbol{C}_{\boldsymbol{h}(\tilde{S})}^{(1)}(\tilde{S}))}{{\rm d}\tilde{S}}\cdot\boldsymbol{z}_{[1]}$, when the $\boldsymbol{C}_{\boldsymbol{h}}^{(j)}(\tilde{S})$'s depend explicitly on $\tilde{S}$. These two additional terms make their way into the final expression of the 1d energy.

The illustration examples in sections 3–5 were simple enough that they could be solved analytically. When this is not possible, the proposed reduction method lends itself naturally to a numerical implementation: by solving numerically a series of elasticity problem over the cross-section, it is possible to build a numerical representation of the various operators $\boldsymbol{A}_{\boldsymbol{h}}$, $\boldsymbol{B}_{\boldsymbol{h}}$ and $\boldsymbol{C}_{\boldsymbol{h}}$, i.e., to evaluate numerically the coefficients of the 1d energy $\Phi^\star$.

This paper was prepared using TeXmacs (van der Hoeven et al., 2013), an outstanding and freely available scientific text editor.

Appendix A. Proof of the main results

In this appendix, we offer a detailed justification of the results announced in §2.

Appendix A.1. Change of microscopic variable

We return to the relaxation problem (2.4) for a prescribed, non-homogeneous distribution of macroscopic strain $\{\boldsymbol{h}(S)\}_S$, and seek the microscopic displacement achieving the optimum of the functional $\Phi[\boldsymbol{h},\boldsymbol{y}]$ in equation (2.2) subject to the constraint $\boldsymbol{q}(\boldsymbol{y}(S))$ in equation (2.3). We seek $\boldsymbol{y}(S)$ in the form (2.8), $\boldsymbol{y}(S) = \boldsymbol{y}_{\boldsymbol{h}(S)} + \boldsymbol{z}(S)$. Since $\boldsymbol{y}_{\boldsymbol{h}(S)}$ satisfies the linear constraint by construction, the new unknown $\boldsymbol{z}(S)$ must satisfy the constraint as well, $\forall S \quad \boldsymbol{q}(\boldsymbol{z}(S)) = \boldsymbol{0}$.

In terms of $\boldsymbol{z}(S)$, the gradients of the original microscopic displacement write

$$\begin{array}{rcl}\boldsymbol{y}'(S) &=& \boldsymbol{h}'(S)\cdot\nabla\boldsymbol{y}_{\boldsymbol{h}(S)} + \boldsymbol{z}'(S)\\ \boldsymbol{y}''(S) &=& \boldsymbol{h}''(S)\cdot\nabla\boldsymbol{y}_{\boldsymbol{h}(S)} + \boldsymbol{h}'(S)\cdot\nabla\boldsymbol{y}_{\boldsymbol{h}(S)}\cdot\boldsymbol{h}'(S) + \boldsymbol{z}''(S)\end{array}$$

where ∇ denotes the gradient with respect to the macroscopic parameter $\boldsymbol{h}$, see equation (2.10). In view of this, the strain appearing in the strain energy in equation (2.2) can be expressed in terms of the new unknown as

$$\boldsymbol{E} = \boldsymbol{e}_{\boldsymbol{h}(S)}(\boldsymbol{h}'(S),\boldsymbol{h}''(S);\boldsymbol{z}(S),\boldsymbol{z}'(S),\boldsymbol{z}''(S)),$$

where $\boldsymbol{e}_{\boldsymbol{h}}(\boldsymbol{h}^\dagger,\boldsymbol{h}^\ddagger;\boldsymbol{z},\boldsymbol{z}^\dagger,\boldsymbol{z}^\ddagger)$ is the strain function introduced in equation (2.9).

Note that the principle of virtual work for the homogeneous solution (2.6) can be rewritten in hindsight using the structure coefficient $\boldsymbol{e}^{00}_{100}$ as

$$\begin{array}{ll} \forall \hat{\boldsymbol{y}} & -\boldsymbol{\Sigma}_{\boldsymbol{h}} \cdot (\boldsymbol{e}^{00}_{100}(\boldsymbol{h}) \cdot \hat{\boldsymbol{y}}) + \boldsymbol{f}_{\boldsymbol{h}} \cdot \boldsymbol{q}(\hat{\boldsymbol{y}}) = 0 \\ \boldsymbol{q}(\boldsymbol{y}_{\boldsymbol{h}}) = \boldsymbol{0}. & \end{array} \tag{A.1}$$

Appendix A.2. Expansion method

Given the distribution of macroscopic strain $\boldsymbol{h}(S)$, the strain energy of the full model is expressed in terms of the corrective displacement $\boldsymbol{z}(S)$ as

$$\Phi[\boldsymbol{h}, \boldsymbol{y}_{\boldsymbol{h}} + \boldsymbol{z}] = \int_0^L W(\boldsymbol{e}_{\boldsymbol{h}(S)}(\boldsymbol{h}'(S), \boldsymbol{h}''(S); \boldsymbol{z}(S), \boldsymbol{z}'(S), \boldsymbol{z}''(S)))\, \mathrm{d}S.$$

This energy must be relaxed with respect to $\boldsymbol{z}$, subject to the constraint

$$\forall S \quad \boldsymbol{q}(\boldsymbol{z}(S)) = \boldsymbol{0}.$$

This relaxation problem is treated by an asymptotic method, which assumes that the prescribed strain $\boldsymbol{h}(S)$ is a slowly varying function of S. Accordingly, we introduce a stretched variable $\tilde{S} = \gamma\, S$ where $\gamma \ll 1$ is a small parameter. We denote by a dot the derivation with respect to the new variable,

$$\dot{f} = \frac{\mathrm{d}f}{\mathrm{d}\tilde{S}}.$$

The assumption of slow axial variations is implemented by requiring that the dependence of the various functions on S encountered so far is replaced with a dependence on the slow variable $\tilde{S}$. This amounts to assuming $\dot{f} = \mathcal{O}(1)$, $\ddot{f} = \mathcal{O}(1)$, etc. while the original derivatives scale as

$$f' = \gamma\, \dot{f} = \mathcal{O}(\gamma) \quad f'' = \gamma^2\, \ddot{f} = \mathcal{O}(\gamma^2) \quad \text{etc.}$$

We seek the microscopic correction as an expansion

$$\boldsymbol{z}(\tilde{S}) = \gamma\, \boldsymbol{z}_{[1]}(\tilde{S}) + \gamma^2\, \boldsymbol{z}_{[2]}(\tilde{S}) + \cdots \tag{A.2}$$

where the absence of any term of order $\gamma^0 = 1$ follows from the observation that in the homogeneous case, corresponding to the formal limit $\gamma \to 0$, we have $\boldsymbol{z}(S) = 0$.

The strain energy to be relaxed can be rescaled as $\tilde{\Phi} = \Phi/\gamma$, where

$$\tilde{\Phi}[\boldsymbol{h}, \boldsymbol{z}] = \int_0^{\tilde{L}} W(\boldsymbol{e}_{\boldsymbol{h}}(\gamma\, \dot{\boldsymbol{h}}(\tilde{S}), \gamma^2\, \ddot{\boldsymbol{h}}(\tilde{S}); \gamma\, \boldsymbol{z}_{[1]}(\tilde{S}) + \gamma^2\, \boldsymbol{z}_{[2]}(\tilde{S}) + \cdots, \gamma^2\, \dot{\boldsymbol{z}}_{[1]}(\tilde{S}) + \cdots, \boldsymbol{0}))\, \mathrm{d}\tilde{S} + \mathcal{O}(\gamma^3), \tag{A.3}$$

and $\tilde{L} = \gamma\, L$, subject to the constraint

$$\forall i \geq 1 \quad \forall \tilde{S} \quad \boldsymbol{q}(\boldsymbol{z}_{[i]}(\tilde{S})) = \boldsymbol{0}. \tag{A.4}$$

We now proceed to derive an expansion of the energy $\tilde{\Phi}$ in powers of γ, and to solve this problem order by order.

Appendix A.3. Strain expansion

The argument $\boldsymbol{e}_{\boldsymbol{h}}$ of W in (A.3) is the strain. It can be expanded as

$$\boldsymbol{e}_{\boldsymbol{h}}(\gamma\, \dot{\boldsymbol{h}}(\tilde{S}), \gamma^2\, \ddot{\boldsymbol{h}}(\tilde{S}); \gamma\, \boldsymbol{z}_{[1]}(\tilde{S}) + \gamma^2\, \boldsymbol{z}_{[2]}(\tilde{S}), \gamma^2\, \dot{\boldsymbol{z}}_{[1]}(\tilde{S}), \boldsymbol{0}) = \boldsymbol{E}_{\boldsymbol{h}(\tilde{S})} + \gamma\, \boldsymbol{e}_{[1]}(\tilde{S}) + \gamma^2\, \boldsymbol{e}_{[2]}(\tilde{S}) + \mathcal{O}(\gamma^3) \tag{A.5}$$

where term of order γ^0 is the homogeneous strain $\boldsymbol{E}_{\boldsymbol{h}(\tilde{S})} = \boldsymbol{E}(\boldsymbol{h}(\tilde{S}), \boldsymbol{0}; \boldsymbol{y}_{\boldsymbol{h}(\tilde{S})}, \boldsymbol{0}, \boldsymbol{0})$ defined in equation (2.7), and the linear and quadratic corrections can be written in terms of the structure coefficients as

$$\begin{array}{rcl} \boldsymbol{e}_{[1]}(\tilde{S}) & = & \boldsymbol{e}^{10}_{000}(\boldsymbol{h}(\tilde{S})) \cdot \dot{\boldsymbol{h}}(\tilde{S}) + \boldsymbol{e}^{00}_{100}(\boldsymbol{h}(\tilde{S})) \cdot \boldsymbol{z}_{[1]}(\tilde{S}) \\ \boldsymbol{e}_{[2]}(\tilde{S}) & = & \frac{1}{2}\,(\dot{\boldsymbol{h}} \cdot \boldsymbol{e}^{20}_{000}(\boldsymbol{h}) \cdot \dot{\boldsymbol{h}} + 2\, \dot{\boldsymbol{h}} \cdot \boldsymbol{e}^{10}_{100}(\boldsymbol{h}) \cdot \boldsymbol{z}_{[1]} + \boldsymbol{z}_{[1]} \cdot \boldsymbol{e}^{00}_{200}(\boldsymbol{h}) \cdot \boldsymbol{z}_{[1]}) \cdots \\ & & \qquad + \boldsymbol{e}^{01}_{000}(\boldsymbol{h}) \cdot \ddot{\boldsymbol{h}} + \boldsymbol{e}^{00}_{010}(\boldsymbol{h}) \cdot \dot{\boldsymbol{z}}_{[1]} + \boldsymbol{e}^{00}_{100}(\boldsymbol{h}) \cdot \boldsymbol{z}_{[2]}. \end{array} \tag{A.6}$$

All the quantities appearing in the right-hand side of $\boldsymbol{e}_{[2]}(\tilde{S})$ must be evaluated at $\tilde{S}$, like those in the right-hand side of $\boldsymbol{e}_{[2]}(\tilde{S})$.

Appendix A.4. Energy expansion

The strain expansion (A.5) can be inserted into the energy in (A.3)

$$\tilde{\Phi}[\boldsymbol{h},\boldsymbol{z}] = \int_0^{\tilde{L}} (W(\boldsymbol{e}_{\boldsymbol{h}(\tilde{S})} + \gamma\, \boldsymbol{e}_{[1]}(\tilde{S}) + \gamma^2\, \boldsymbol{e}_{[2]}(\tilde{S})) + \mathcal{O}(\gamma^3))\, \mathrm{d}\tilde{S}$$

This yields an expansion of the energy as

$$\tilde{\Phi}[\boldsymbol{h},\boldsymbol{z}] = \tilde{\Phi}_{[0]}[\boldsymbol{h}] + \gamma\, \tilde{\Phi}_{[1]}[\boldsymbol{h}] + \gamma^2\, \tilde{\Phi}_{[2]}[\boldsymbol{h},\boldsymbol{z}_{[1]}] + \cdots \tag{A.7}$$

where the first orders in the expansion read

$$\begin{array}{rcl} \tilde{\Phi}_{[0]}[\boldsymbol{h}] & = & \int_0^{\tilde{L}} W_{\mathrm{hom}}(\boldsymbol{h}(\tilde{S}))\, \mathrm{d}\tilde{S} \\ \tilde{\Phi}_{[1]}[\boldsymbol{h}] & = & \int_0^{\tilde{L}} \boldsymbol{\Sigma}_{\boldsymbol{h}(\tilde{S})} \cdot \boldsymbol{e}_{[1]}(\tilde{S})\, \mathrm{d}\tilde{S} \\ \tilde{\Phi}_{[2]}[\boldsymbol{h},\boldsymbol{z}_{[1]}] & = & \int_0^{\tilde{L}} \left(\frac{1}{2}\, \boldsymbol{e}_{[1]}(\tilde{S}) \cdot \boldsymbol{K}_{\boldsymbol{h}(\tilde{S})} \cdot \boldsymbol{e}_{[1]}(\tilde{S}) + \boldsymbol{\Sigma}_{\boldsymbol{h}(\tilde{S})} \cdot \boldsymbol{e}_{[2]}(\tilde{S}) \right) \mathrm{d}\tilde{S}. \end{array}$$

Our notation anticipates on the fact that $\tilde{\Phi}_{[1]}$ does not depend on $\boldsymbol{z}$, and that $\tilde{\Phi}_{[2]}$ depends on $\boldsymbol{z}$ through its dominant contribution $\boldsymbol{z}_{[1]}$ only, as we prove in the next section.

Appendix A.5. Rearranging the energy contributions

Using the operator $\boldsymbol{A}_{\boldsymbol{h}}$ introduced in equation (2.12), the energy contribution $\tilde{\Phi}_{[1]}$ can be written as

$$\tilde{\Phi}_{[1]}[\boldsymbol{h}] = \int_0^{\tilde{L}} (\boldsymbol{A}_{\boldsymbol{h}(\tilde{S})} \cdot \dot{\boldsymbol{h}}(\tilde{S}) + \boldsymbol{\Sigma}_{\boldsymbol{h}(\tilde{S})} \cdot (\boldsymbol{e}^{00}_{100}(\boldsymbol{h}(\tilde{S})) \cdot \boldsymbol{z}_{[1]}(\tilde{S})))\, \mathrm{d}\tilde{S}.$$

The second term in the integrand can be simplified by using the principle of virtual work for homogeneous solutions (A.1): setting the virtual motion as $\hat{\boldsymbol{y}} = \boldsymbol{y}_{\boldsymbol{h}(\tilde{S})}$, one has $\boldsymbol{\Sigma}_{\boldsymbol{h}(\tilde{S})} \cdot (\boldsymbol{e}^{00}_{100}(\boldsymbol{h}(\tilde{S})) \cdot \boldsymbol{y}_{\boldsymbol{h}(\tilde{S})}) = \boldsymbol{f}_{\boldsymbol{h}(\tilde{S})} \cdot \boldsymbol{q}(\boldsymbol{y}_{\boldsymbol{h}(\tilde{S})}) = 0$ since $\boldsymbol{y}_{\boldsymbol{h}(\tilde{S})}$ satisfies the constraint $\boldsymbol{q}$. This shows that the second term in the integrand above vanishes, and that $\tilde{\Phi}_{[1]}[\boldsymbol{h}]$ is actually independent of the microscopic displacement $\boldsymbol{z}$, as anticipated in our notation,

$$\tilde{\Phi}_{[1]}[\boldsymbol{h}] = \int_0^{\tilde{L}} \boldsymbol{A}_{\boldsymbol{h}(\tilde{S})} \cdot \dot{\boldsymbol{h}}(\tilde{S})\, \mathrm{d}\tilde{S}.$$

Most structures are invariant by the reflection $S \leftarrow (-S)$, which implies that the operator $\boldsymbol{A}_{\boldsymbol{h}}$, as well as the first-order correction to the energy $\tilde{\Phi}_{[1]}[\boldsymbol{h}]$, vanish. This makes it important to determine the expansion of the energy to second order.

At order γ^2, we have

$$\tilde{\Phi}_{[2]}[\boldsymbol{h},\boldsymbol{z}_{[1]}] = \int_0^{\tilde{L}} \left(\frac{1}{2}\, \boldsymbol{e}_{[1]}(\tilde{S}) \cdot \boldsymbol{K}_{\boldsymbol{h}(\tilde{S})} \cdot \boldsymbol{e}_{[1]}(\tilde{S}) + \boldsymbol{\Sigma}_{\boldsymbol{h}(\tilde{S})} \cdot \boldsymbol{e}_{[2]}(\tilde{S}) \right) \mathrm{d}\tilde{S}$$

Inserting the expression of $\boldsymbol{e}_{[1]}$ and $\boldsymbol{e}_{[2]}$ in the integrand, and using the operators defined in (2.12), we can rewrite this as

$$\tilde{\Phi}_{[2]}[\boldsymbol{h},\boldsymbol{z}_{[1]}] = \int_0^{\tilde{L}} \left(\begin{array}{l} \boldsymbol{C}^{(0)}_{\boldsymbol{h}} \cdot \ddot{\boldsymbol{h}} + \frac{\mathrm{d}(\boldsymbol{C}^{(0)}_{\boldsymbol{h}(\tilde{S})})}{\mathrm{d}\tilde{S}} \cdot \dot{\boldsymbol{h}} + \boldsymbol{C}^{(1)}_{\boldsymbol{h}} \cdot \dot{\boldsymbol{z}}_{[1]} + \frac{\mathrm{d}(\boldsymbol{C}^{(1)}_{\boldsymbol{h}(\tilde{S})})}{\mathrm{d}\tilde{S}} \cdot \boldsymbol{z}_{[1]} \cdots \\ + \frac{1}{2}\, \dot{\boldsymbol{h}} \cdot \boldsymbol{B}^{(0)}_{\boldsymbol{h}} \cdot \dot{\boldsymbol{h}} + \dot{\boldsymbol{h}} \cdot \boldsymbol{B}^{(1)}_{\boldsymbol{h}} \cdot \boldsymbol{z}_{[1]} + \frac{1}{2}\, \boldsymbol{z}_{[1]} \cdot \boldsymbol{B}^{(2)}_{\boldsymbol{h}} \cdot \boldsymbol{z}_{[1]} \cdots \\ + \boldsymbol{\Sigma}_{\boldsymbol{h}} \cdot (\boldsymbol{e}^{00}_{100}(\boldsymbol{h}) \cdot \boldsymbol{z}_{[2]}) \end{array} \right) \mathrm{d}\tilde{S} \tag{A.8}$$

where all quantities in the integrand must evaluated at $\tilde{S}$, namely $\boldsymbol{h} = \boldsymbol{h}(\tilde{S})$, $\dot{\boldsymbol{h}} = \dot{\boldsymbol{h}}(\tilde{S})$, $\boldsymbol{z}_{[i]} = \boldsymbol{z}_{[i]}(\tilde{S})$ and $\dot{\boldsymbol{z}}_{[1]} = \dot{\boldsymbol{z}}_{[1]}(\tilde{S})$. In this expression, we have made appear the term $\frac{\mathrm{d}(\boldsymbol{C}^{(0)}_{\boldsymbol{h}(\tilde{S})})}{\mathrm{d}\tilde{S}} \cdot \dot{\boldsymbol{h}}(\tilde{S}) = \dot{\boldsymbol{h}}(\tilde{S}) \cdot \nabla \boldsymbol{C}^{(0)}_{\boldsymbol{h}(\tilde{S})} \cdot \dot{\boldsymbol{h}}(\tilde{S})$,

which cancels out with the last term introduced in the definition of $\frac{1}{2}\,\dot{\boldsymbol{h}}\cdot\boldsymbol{B}^{(0)}_{\boldsymbol{h}}\cdot\dot{\boldsymbol{h}}$, see equation (2.12). The same holds for $\frac{\mathrm{d}(\boldsymbol{C}^{(1)}_{\boldsymbol{h}(\tilde{S})})}{\mathrm{d}\tilde{S}}\cdot\boldsymbol{z}_{[1]}$ and the last term in $\dot{\boldsymbol{h}}\cdot\boldsymbol{B}^{(1)}_{\boldsymbol{h}}\cdot\boldsymbol{z}_{[1]}$.

In addition, the last term in the integrand of $\tilde{\Phi}_{[2]}[\boldsymbol{h},\boldsymbol{z}_{[1]}]$ cancels by the same argument as earlier, i.e., using the homogeneous principle of virtual work (A.1) and the constraint (A.4) at second order. As a result, $\tilde{\Phi}_{[2]}$ depends on $\boldsymbol{z}_{[1]}$ but not on $\boldsymbol{z}_{[2]}$, as anticipated in our notation. Noting that the terms on the first line in the integrand form an exact derivative, and can be integrated, we have

$$\tilde{\Phi}_{[2]}[\boldsymbol{h},\boldsymbol{z}_{[1]}]=[\boldsymbol{C}^0_{\boldsymbol{h}}\cdot\dot{\boldsymbol{h}}+\boldsymbol{C}^1_{\boldsymbol{h}}\cdot\boldsymbol{z}_{[1]}]_0^{\tilde{L}}+\int_0^{\tilde{L}}\left(\frac{1}{2}\,\dot{\boldsymbol{h}}\cdot\boldsymbol{B}^{(0)}_{\boldsymbol{h}}\cdot\dot{\boldsymbol{h}}+\dot{\boldsymbol{h}}\cdot\boldsymbol{B}^{(1)}_{\boldsymbol{h}}\cdot\boldsymbol{z}_{[1]}+\frac{1}{2}\,\boldsymbol{z}_{[1]}\cdot\boldsymbol{B}^{(2)}_{\boldsymbol{h}}\cdot\boldsymbol{z}_{[1]}\right)\mathrm{d}\tilde{S}\quad(\mathrm{A}.9)$$

where all the quantities in the integrand side are implicitly evaluated at $\tilde{S}$ in our notation.

The expansion of the energy $\Phi[\boldsymbol{h},\boldsymbol{y}_{\boldsymbol{h}}+\boldsymbol{z}]$ in non-scaled form, announced earlier in equation (2.13), is readily obtained by inserting into equation (A.7) the expressions of $\tilde{\Phi}_{[0]}$, $\tilde{\Phi}_{[1]}$ and $\tilde{\Phi}_{[2]}$ just derived, and restoring the original (scaled) gradients $\boldsymbol{h}'$, $\boldsymbol{h}''$, $\boldsymbol{z}'$ and $\boldsymbol{z}''$, as well as the unscaled longitudinal coordinate S.

Appendix A.6. Dominant order correction found by a local problem

We now proceed to minimize the energy (A.3) under the constraint (A.4) order by order, using the expansion of $\tilde{\Phi}[\boldsymbol{h},\boldsymbol{z}]$ just found. Thanks to the integration by parts, the dependence of the strain energy $\tilde{\Phi}_{[2]}[\boldsymbol{h},\boldsymbol{z}_{[1]}]$ on the axial gradient $\boldsymbol{z}'_{[1]}$ of the corrective displacement has been removed. Therefore, in every cross-section $\tilde{S}$, $\boldsymbol{z}_{[1]}(\tilde{S})$ is the solution of a *local* optimization problem: $\boldsymbol{z}_{[1]}(\tilde{S})$ makes stationary the quantity $\boldsymbol{B}^{(1)}_{\boldsymbol{h}}\cdot\boldsymbol{z}_{[1]}+\frac{1}{2}\,\boldsymbol{z}_{[1]}\cdot\boldsymbol{B}^{(2)}_{\boldsymbol{h}}\cdot\boldsymbol{z}_{[1]}$ among all $\boldsymbol{z}$'s satisfying the constraint $\boldsymbol{q}(\boldsymbol{z})=\boldsymbol{0}$. This leads to the variational problem stated in equation (2.14), where we use the notation $\boldsymbol{z}_{\mathrm{opt}}=\gamma\,\boldsymbol{z}_{[1]}$ for the dominant contribution to the correction $\boldsymbol{z}$, see equation (A.2), and $\boldsymbol{f}_{\mathrm{opt}}=\gamma\,\boldsymbol{f}_{[1]}$ for the scaled Lagrange multiplier. In terms of $\boldsymbol{z}_{[1]}$, the variational problem can be written equivalently as $\forall\hat{\boldsymbol{z}}\quad\dot{\boldsymbol{h}}(\tilde{S})\cdot\boldsymbol{B}^{(1)}_{\boldsymbol{h}(\tilde{S})}\cdot\hat{\boldsymbol{z}}+\boldsymbol{z}_{[1]}(\tilde{S})\cdot\boldsymbol{B}^{(2)}_{\boldsymbol{h}(\tilde{S})}\cdot\hat{\boldsymbol{z}}-\boldsymbol{f}_{[1]}(\tilde{S})\cdot\boldsymbol{q}(\hat{\boldsymbol{z}})=0$ and $\boldsymbol{q}(\boldsymbol{z}_{[1]}(\tilde{S}))=\boldsymbol{0}$.

Appendix A.7. Relaxed energy

By using the particular virtual motion $\hat{\boldsymbol{z}}=\boldsymbol{z}_{[1]}(\tilde{S})$ in the above variational problem, we obtain the identity

$$\dot{\boldsymbol{h}}(\tilde{S})\cdot\boldsymbol{B}^{(1)}_{\boldsymbol{h}(\tilde{S})}\cdot\boldsymbol{z}_{[1]}(\tilde{S})=-\boldsymbol{z}_{[1]}(\tilde{S})\cdot\boldsymbol{B}^{(2)}_{\boldsymbol{h}(\tilde{S})}\cdot\boldsymbol{z}_{[1]}(\tilde{S}).$$

When the optimal displacement $\boldsymbol{z}^{\mathrm{opt}}_{[1]}$ is inserted into $\tilde{\Phi}_{[2]}[\boldsymbol{h},\boldsymbol{z}_{[1]}]$ in equation (A.9), and this identity is used, we obtain the second-order contribution to the relaxed energy as

$$\tilde{\Phi}^{\star}_{[2]}[\boldsymbol{h}]=\tilde{\Phi}_{[2]}[\boldsymbol{h},\boldsymbol{z}^{\mathrm{opt}}_{[1]}]=[\boldsymbol{C}^0_{\boldsymbol{h}}\cdot\dot{\boldsymbol{h}}+\boldsymbol{C}^1_{\boldsymbol{h}}\cdot\boldsymbol{z}^{\mathrm{opt}}_{[1]}]_0^{\tilde{L}}+\int_0^{\tilde{L}}\left(\frac{1}{2}\,\dot{\boldsymbol{h}}\cdot\boldsymbol{B}^{(0)}_{\boldsymbol{h}}\cdot\dot{\boldsymbol{h}}-\frac{1}{2}\,\boldsymbol{z}_{[1]}\cdot\boldsymbol{B}^{(2)}_{\boldsymbol{h}}\cdot\boldsymbol{z}^{\mathrm{opt}}_{[1]}\right)\mathrm{d}\tilde{S}.$$

This yields the final expressions (2.16–2.17) of the relaxed model.

Appendix B. Detailed calculations for the nonlinear cylinder

Appendix B.1. Analysis of homogeneous solutions

In this section, we provide a detailed analysis of the homogeneous solutions for the hyperelastic cylinder, with the aim to justify the main results announced in section 5.3.

The map of strain for homogeneous solutions writes, from equation (2.5) and (5.1),

$$\tilde{\boldsymbol{E}}(\boldsymbol{h},\boldsymbol{y})=\begin{pmatrix}\left\{\frac{1}{2}\,(h_1^2-1)\right\}_T\\ \left\{\frac{1}{2}\,((\partial_T y_1)^2+(\partial_T y_2)^2-1)\right\}_T\\ \left\{\frac{1}{2}\,h_1\,\partial_T y_1\right\}_T\\ \left\{\frac{1}{2}\,\left(\left(\frac{y_2}{T}\right)^2-1\right)\right\}_T\end{pmatrix}.$$

In view of the material symmetries, we seek equi-biaxial solutions in the particular form $y_1 = \{0\}_T$ and $y_2 = \{\mu\, T\}_T$. Then,

$$\tilde{\boldsymbol{E}}(\boldsymbol{h},\boldsymbol{y}) = \tilde{\boldsymbol{E}}(\boldsymbol{h},(\{0\}_T,\{\mu\, T\}_T)) = \begin{pmatrix} \left\{\frac{1}{2}\,(h_1^2-1)\right\}_T \\ \left\{\frac{1}{2}\,(\mu^2-1)\right\}_T \\ \{0\}_T \\ \left\{\frac{1}{2}\,(\mu^2-1)\right\}_T \end{pmatrix} \quad \frac{\partial \tilde{\boldsymbol{E}}}{\partial \boldsymbol{y}}(\boldsymbol{h},(\{0\}_T,\{\mu\, T\}_T))\cdot\hat{\boldsymbol{y}} = \begin{pmatrix} \{0\}_T \\ \{\mu\, \partial_T \hat{y}_2\}_T \\ \left\{\frac{1}{2}\, h_1\, \partial_T \hat{y}_1\right\}_T \\ \left\{\frac{\mu\, \hat{y}_2}{T}\right\}_T \end{pmatrix}.$$

For this type of strain, the material symmetry warrants $\overline{\Sigma}_{ST} = 0$ and $\overline{\Sigma}_{TT} = \overline{\Sigma}_{\Theta\Theta}$. We denote the longitudinal stress as $\overline{\Sigma}_{\parallel}(h_1,\mu) = \overline{\Sigma}_{SS}$ and the isotropic transverse stress as $\overline{\Sigma}_{\perp}(h_1,\mu) = \overline{\Sigma}_{TT} = \overline{\Sigma}_{\Theta\Theta}$. Then, the first variation of the density of strain energy reads

$$\begin{aligned} \tfrac{\mathrm{d}W}{\mathrm{d}\boldsymbol{E}}(\tilde{\boldsymbol{E}}(\boldsymbol{h},\boldsymbol{y}))\cdot\delta\boldsymbol{E} &= \int_0^\rho \begin{pmatrix} \overline{\Sigma}_{SS} \\ \overline{\Sigma}_{TT} \\ 2\,\overline{\Sigma}_{ST} \\ \overline{\Sigma}_{\Theta\Theta} \end{pmatrix} \cdot \begin{pmatrix} \delta E_1(T) \\ \delta E_2(T) \\ \delta E_3(T) \\ \delta E_4(T) \end{pmatrix} 2\,\pi\, T\,\mathrm{d}T \\ &= \int_0^\rho (\overline{\Sigma}_{\parallel}(h_1,\mu)\,\delta E_1(T) + \overline{\Sigma}_{\perp}(h_1,\mu)\,(\delta E_2(T)+\delta E_4(T)))\,2\,\pi\, T\,\mathrm{d}T. \end{aligned}$$

By combining these equations with equation (2.6), we obtain a principle of virtual work for the homogeneous radial displacement $y_2^{\boldsymbol{h}} = \{\mu_{\boldsymbol{h}}\, T\}_T$ as

$$\forall \hat{y}_1, \hat{y}_2 \quad \int_0^\rho \left[f_1^{\boldsymbol{h}}\, \hat{y}_1(T) - \mu\, \overline{\Sigma}_{\perp}(h_1,\mu_{\boldsymbol{h}})\, \left(\frac{\hat{y}_2(T)}{T} + \partial_T \hat{y}_2(T) \right) \right] 2\,\pi\, T\,\mathrm{d}T = 0$$

It can be seen that the Lagrange multiplier is zero, $f_1^{(h_1)} = 0$, which is a consequence of the fact that our trial function satisfies the constraint already. The other term in the integrand above can be rewritten as $\int_0^\rho [-2\,\pi\,\mu\,\overline{\Sigma}_{\perp}(h_1,\mu_{\boldsymbol{h}})\,\partial_T(T\,\hat{y}_2)]\,\mathrm{d}T = -2\,\pi\,\mu\,\overline{\Sigma}_{\perp}(h_1,\mu_{\boldsymbol{h}})\rho\,\hat{y}_2(\rho)$ and so the principle of virtual work yields the equation $\overline{\Sigma}_{\perp}(h_1,\mu_{(h_1)}) = 0$ as announced in equation (5.6).

We proceed to present a derivation of the stress and the tangent moduli in the homogeneous solution.

The stress is found by identifying the first variation of the elastic potential $\overline{W}(E_1(S), E_3^2(S), E_2(S) + E_4(S), E_2^2(S) + E_4^2(S), E_2(S)\,E_3^2(S))$, namely

$$\delta\overline{W} = \partial_1\overline{W}\,\delta E_1 + 2\,E_3\,\partial_2\overline{W}\,\delta E_3 + (\delta E_2 + \delta E_4)\,\partial_3\overline{W} + 2\,(E_2\,\delta E_2 + E_4\,\delta E_4)\,\partial_4\overline{W} + (E_3^2\,\delta E_2 + 2\,E_2\,E_3\,\delta E_3)\,\partial_5\overline{W}.$$

Identifying the stress components with the definition of Piola-Kirchhoff stress from the general theory of elasticity, $\delta\overline{W} = \sum_{IJ}\overline{\Sigma}_{IJ}\,\delta\overline{E}_{IJ}$, using of the definition of the $\overline{E}_{IJ}$'s in terms of $(E_1,\ldots,E_4)$ (see below equation (5.1)) and evaluating these stress components in the homogeneous solution yields the equation (5.5).

The tangent moduli are found similarly, by identifying the second variation of the elastic potential

$$\delta^2\overline{W} = \partial_{11}\overline{W} \times (\delta E_1)^2 + \ldots$$

with the definition of the tangent moduli from the general theory of elasticity, $\delta^2\overline{W} = \sum_{IJLM}\overline{K}_{IJ}^{LM}\,\delta\overline{E}_{IJ}\,\delta\overline{E}_{LM}$. This yields the expression of $\overline{K}_{ST}^{ST}$ given in equation (5.7), together with the additional tangent elastic moduli

$$\begin{aligned} \overline{K}_{TT}^{TT} &= 2\,\partial_4\overline{W} + \overline{K}_{TT}^{\Theta\Theta} \\ \overline{K}_{TT}^{\Theta\Theta} &= \partial_{33}\overline{W} + 2\,(\mu_{(h_1)}^2 - 1)\,\partial_{34}\overline{W} + (\mu_{(h_1)}^2-1)^2\,\partial_{44}\overline{W}. \end{aligned}$$

The factor $1/4$ in equation (5.7) comes from the fact that there are four possible sets of indices (I,J,L,M) such that $\delta\overline{E}_{IJ}\,\delta\overline{E}_{LM} = (\delta\overline{E}_{ST})^2$.

Appendix B.2. Strain function in terms of the microscopic correction

The change of microscopic unknown is carried out by setting $\boldsymbol{y}(S) = \boldsymbol{y_h}(S) + \boldsymbol{z}(S)$, that is $y_1 = z_1$ and $y_2 = y_2^{(h_1)} + z_2 = \mu_{(h_1)}\, T + z_2$. A strain function $\boldsymbol{e_h}$ defined in terms of the new unknown $\boldsymbol{z}$ has been introduced in equation (2.9). Inserting the expression of $\boldsymbol{E}$ from equation (5.4) relevant to nonlinear elastic cylinder yields

$$\boldsymbol{e_h}(\boldsymbol{h}^\dagger, \boldsymbol{h}^\ddagger; \boldsymbol{z}, \boldsymbol{z}^\dagger, \boldsymbol{z}^\ddagger) = \begin{pmatrix} \left\{ \frac{1}{2} \left((h_1 + z_1^\dagger(T))^2 + (h_1^\dagger \nabla \mu_{(h_1)}\, T + z_2^\dagger(T))^2 - 1 \right) \right\}_T \\ \left\{ \frac{1}{2} \left((\partial_T z_1(T))^2 + (\mu_{(h_1)} + \partial_T z_2(T))^2 - 1 \right) \right\}_T \\ \left\{ \frac{1}{2} \left((h_1 + z_1^\dagger(T))\, \partial_T z_1(T) + (h_1^\dagger \nabla \mu_{(h_1)}\, T + z_2^\dagger(T))\, (\mu_{(h_1)} + \partial_T z_2(T)) \right) \right\}_T \\ \left\{ \frac{1}{2} \left(\left(\mu_{(h_1)} + \frac{z_2(T)}{T} \right)^2 - 1 \right) \right\}_T \end{pmatrix}.$$

Calculating the Taylor expansion of $\boldsymbol{e_h}$ about a homogeneous solution, i.e., for small $\boldsymbol{h}^\dagger$, $\boldsymbol{h}^\ddagger$, $\boldsymbol{z}$, $\boldsymbol{z}^\dagger$ and $\boldsymbol{z}^\ddagger$, we can then identify the coefficients in this expansion with the structure coefficients introduced in equation (2.11).

Appendix B.3. Corrective displacement

In this section, we solve the local optimization problem for the nonlinear cylinder in traction. We start from the expressions of the operators $\boldsymbol{B}_{\boldsymbol{h}}^{(1)}$ and $\boldsymbol{B}_{\boldsymbol{h}}^{(2)}$ obtained in equation (5.9). As the operator $\boldsymbol{B}_{\boldsymbol{h}}^{(2)}$ does not couple the unknowns $z_1(T)$ and $z_2(T)$, the optimization problem for $\boldsymbol{z}$ obtained in equation (2.14) splits into a problem for the axial corrective displacement z_1

$$\begin{cases} \forall \hat{z}_1 \quad \boldsymbol{h}'(S) \cdot \boldsymbol{B}_{\boldsymbol{h}(S)}^{(1)} \cdot (\hat{z}_1, \boldsymbol{0}) + \left(z_1^{\text{opt}}, \boldsymbol{0} \right) \cdot \boldsymbol{B}_{\boldsymbol{h}(S)}^{(2)} \cdot (\hat{z}_1, \boldsymbol{0}) - \boldsymbol{f}_{\text{opt}}(S) \cdot \boldsymbol{q}((\hat{z}_1, \boldsymbol{0})) = 0 \\ \boldsymbol{q}\left(z_1^{\text{opt}}, \boldsymbol{0} \right) = 0, \end{cases} \tag{B.1}$$

and a problem for the radial corrective displacement z_2,

$$\left\{ \forall \hat{z}_2 \quad \boldsymbol{h}'(S) \cdot \boldsymbol{B}_{\boldsymbol{h}(S)}^{(1)} \cdot (\boldsymbol{0}, \hat{z}_2) + \left(\boldsymbol{0}, z_2^{\text{opt}} \right) \cdot \boldsymbol{B}_{\boldsymbol{h}(S)}^{(2)} \cdot (\boldsymbol{0}, \hat{z}_2) = 0. \right.$$

In the latter, the first term $\boldsymbol{h}'(S) \cdot \boldsymbol{B}_{\boldsymbol{h}(S)}^{(1)} \cdot (\boldsymbol{0}, \hat{z}_2)$ vanishes in view of the definition of $\boldsymbol{B}_{\boldsymbol{h}}^{(1)}$ in equation (5.9). The solution for the corrective radial displacement is therefore zero,

$$z_2^{\text{opt}} = \{0\}_T.$$

Observe that the second term in the right-hand side of the definition of $\boldsymbol{B}_{\boldsymbol{h}}^{(1)}$ in equation (5.9) is zero, as it is proportional to the constraint $\boldsymbol{q}\left(z_1^{\text{opt}}, \boldsymbol{0} \right) = \int_0^\rho z_1^{\text{opt}}(T)\, 2\,\pi\, T\, \mathrm{d}T$. Inserting the expressions of the operators $\boldsymbol{B}_{\boldsymbol{h}}^{(1)}$ and $\boldsymbol{B}_{\boldsymbol{h}}^{(2)}$ from equation (5.9), we can rewrite the variational problem (B.1) as

$$\forall \hat{z}_1 \quad \int_0^\rho \left([h_1\, h_1^{'}\, \overline{K}_{ST}^{ST}\, \mu_{(h_1)}\, \nabla \mu_{(h_1)}]\, T + [h_1^2\, \overline{K}_{ST}^{ST}]\, \partial_T z_1^{\text{opt}}(T) \right) \partial_T \hat{z}_1(T)\, 2\,\pi\, T\, \mathrm{d}T \cdots + \left[-\tilde{f}_1^{\text{opt}} \right] \int_0^\rho \hat{z}_1\, 2\,\pi\, T\, \mathrm{d}T = 0$$

where we have made appear a new Lagrange multiplier $\tilde{f}_1^{\text{opt}} = f_1^{\text{opt}} - h_1^\dagger \frac{\mathrm{d}(\overline{\Sigma}_\parallel(h_1, \mu_{(h_1)})\, h_1)}{\mathrm{d}h_1}$.

To solve this equation, we rewrite it in compact form as

$$\forall \hat{z}_1 \quad \int_0^\rho \left(a\, T + b\, \partial_T z_1^{\text{opt}} \right) \partial_T \hat{z}_1\, 2\,\pi\, T\, \mathrm{d}T + d \int_0^\rho \hat{z}_1\, 2\,\pi\, T\, \mathrm{d}T = 0,$$

where the coefficients a, b, d are identified with the square brackets in the equation above. An integration by parts yields

$$\forall \hat{z}_1 \quad \left[2\,\pi\,T\,\left(a\,T + b\,\partial_T z_1^{\rm opt}\right)\,\hat{z}_1\right]_0^\rho - \int_0^\rho \partial_T \left[2\,\pi\,T\,\left(a\,T + b\,\partial_T z_1^{\rm opt} - d\,\frac{T}{2}\right)\right]\,\hat{z}_1\,{\rm d}T = 0$$

The solution is that $T\,\left(a\,T + b\,\partial_T z_1^{\rm opt} - d\,\frac{T}{2}\right)$ is a constant, which is found using of the boundary conditions as

$$T\,\left(a\,T + b\,\partial_T z_1^{\rm opt} - d\,\frac{T}{2}\right) = -\frac{d\,\rho^2}{2}.$$

We conclude $\partial_T z_1^{\rm opt} = \frac{T}{b}\,\left(\frac{d}{2} - a\right) - \frac{d\,\rho^2}{2\,b}\,\frac{1}{T}$. The Lagrange multiplier $d = \left[-\tilde{f}_1^{\rm opt}\right]$ must be chosen so as to remove the logarithmic divergence for $T \to 0$: this yields $d = 0$. We can integrate the remaining terms and set the constant of integration such that the average constraint $q_1\left(z_1^{\rm opt}\right) = 0$ is satisfied: the result is $z_1^{\rm opt}(T) = -\frac{a}{2\,b}\,\left(T^2 - \frac{\rho^2}{2}\right)$. In terms of the original quantities, the solution for the axial correction to the displacement writes, after simplification, $z_1^{\rm opt}(T) = -\frac{a}{2\,b}\,\left(T^2 - \frac{\rho^2}{2}\right) = -\frac{1}{2}\,\frac{\mu_{(h1)}\,\nabla\mu_{(h_1)}}{h_1}\,h_1'\,\left(T^2 - \frac{\rho^2}{2}\right)$. This can be rewritten as

$$z_1^{\rm opt} = \left\{-\frac{1}{2}\,\frac{\mu_{(h1)}\,\nabla\mu_{(h_1)}}{h_1}\,\left(T^2 - \frac{\rho^2}{2}\right)\right\}_T\,h_1',$$

as captured in equation (5.10).

Acerbi, E., Buttazzo, G., Percivale, D., 1991. A variational definition of the strain energy for an elastic string. Journal of Elasticity 25, 137–148.

Agostiniani, V., DeSimone, A., Koumatos, K., 2016. Shape programming for narrow ribbons of nematic elastomers, arxiv 1603.02088v1.

Audoly, B., Hutchinson, J. W., 2016. Analysis of necking based on a one-dimensional model. Journal of the Mechanics and Physics of Solids 97, 68–91.

Bardenhagen, S., Triantafyllidis, N., 1994. Derivation of higher order gradient continuum theories in 2,3-d non-linear elasticity from periodic lattice models. Journal of the Mechanics and Physics of Solids 42 (1), 111–139.

Barenblatt, G., Joseph, D. (Eds.), 1997. Collected Papers of R.S. Rivlin. Springer, New York, Ch. Stability of an elastic material.

Bermudez, A., Viaño, J. M., 1984. Une justification des équations de la thermoélasticité des poutres à section variable par des méthodes asymptotiques. Modélisation Mathématqiue et Analyse Numérique 18, 347–376.

Buannic, N., Cartaud, P., 2000. Higher-order effective modeling of periodic heterogeneous beams. I. Asymptotic expansion method. International Journal of Solids and Structures 38, 7139–7161.

Calladine, C. R., 1983. Theory of shell structures. Cambridge University Press.

Cimetière, A., Geymonat, G., Le Dret, H., Raoult, A., Tutek, Z., 1988. Asymptotic theory and analysis for displacements and stress distribution in nonlinear elastic straight slender rods. Journal of Elasticity 19, 111–161.

Coleman, B. D., Newman, D. C., 1988. On the rheology of cold drawing. I. elastic materials. Journal of Polymer Science: Part B: Polymer Physics 26, 1801–1822.

Freddi, L., Hornung, P., Mora, M.-G., Paroni, R., 2016. A variational model for anisotropic and naturally twisted ribbons. SIAM Journal on Mathematical Analysis 48 (6), 3883–3906.

Freddi, L., Morassi, A., Paroni, R., 2004. Thin-walled beams: the case of the rectangular cross-section. Journal of Elasticity 76 (1), 45–66.

Fu, Y. B., Pearce, S. P., Liu, K. K., 2008. Post-bifurcation analysis of a thin-walled hyperelastic tube under inflation. International Journal of Non-Linear Mechanics 43 (8), 697–706.

Geymonat, G., Krasucki, F., Serpilli, M., 2018. Asymptotic derivation of linear plate model for soft ferromagnetic material. Chinese Annals of Mathematics, Series B 39 (3), 451–460.

G'Sell, C., Aly-Helal, N. A., Jonas, J. J., 1983. Effect of stress triaxiality on neck propagation during the tensile stretching of solid polymers. Journal of Materials Science 18, 1731–1742.

Hamdouni, A., Millet, O., 2006. An asymptotic non-linear model for thin-walled rods with strongly curved open cross-section. International Journal of Non-Linear Mechanics 41 (3), 396–416.

Kyriakides, S., Chang, Y.-C., 1990. On the inflation of a long elastic tube in the presence of axial load. International Journal of Solids and Structures 26 (9–10), 975–991.

Kyriakides, S., Chang, Y.-C., 1991. The initiation and propagation of a localized instability in an inflated elastic tube. International Journal of Solids and Structures 27 (9), 1085–1111.

Lestringant, C., Audoly, B., 2017. Elastic rods with incompatible strain: macroscopic versus microscopic buckling. Journal of the Mechanics and Physics of Solids 103, 40–71.

Lestringant, C., Audoly, B., 2018. A diffuse interface model for the analysis of propagating bulges in cylindrical balloons. Proceedings of the Royal Society A: Mathematical, Physical and Engineering Sciences 474, 20180333.
Liu, J., Huang, J., Su, T., Bertoldi, K., Clarke, D., 2014. Structural transition from helices to hemihelices. PLoS ONE 9 (4), e93183.
Mahadevan, L., Vaziri, A., Das, M., 2007. Persistence of a pinch in a pipe. Europhysics Letters 77 (4), 40003.
Marigo, J.-J., Meunier, N., 2006. Hierarchy of one-dimensional models in nonlinear elasticity. Journal of Elasticity 83, 1–28.
Matsuo, E. S., Tanaka, T., 1992. Patterns in shrinking gels. Nature 368, 1735.
Mora, S., Phou, T., Fromental, J.-M., Pismen, L. M., Pomeau, Y., Nov 2010. Capillarity driven instability of a soft solid. Physical Review Letters 105, 214301.
Ogden, R. W., 1972. Large deformation isotropic elasticity-on the correlation of theory and experiment for incompressible rubber-like solids. Proceedings of the Royal Society A: Mathematical, Physical and Engineering Science 326, 565–584.
Pearce, S. P., Fu, Y. B., 2010. Characterization and stability of localized bulging/necking in inflated membrane tubes. IMA Journal of Applied Mathematics 75, 581–602.
Picault, E., Bourgeois, S., Cochelin, B., Guinot, F., 2016. A rod model with thin-walled flexible cross-section: Extension to 3D motions and application to 3D foldings of tape springs. International Journal of Solids and Structures 84, 64–81.
Sadowsky, M., 1930. Ein elementarer Beweis für die Existenz eines abwickelbaren Möbiusschen Bandes und die Zurückführung des geometrischen Problems auf ein Variationsproblem. In: Sitzungsberichte der Preussischen Akademie der Wissenschaften, physikalisch-mathematische Klasse, 17. Juli 1930, Mitteilung vom 26. Juni. pp. 412–415.
Sanchez-Hubert, J., Sanchez Palencia, E., 1999. Statics of curved rods on account of torsion and flexion. European Journal of Mechanics. A. Solids 18, 365–390.
Seffen, K. A., Pellegrino, S., 1999. Deployment dynamics of tape springs. Proceedings of the Royal Society of London. Series A: Mathematical, Physical and Engineering Sciences 455 (1983), 1003–1048.
Trabucho, L., Viaño, J. M., 1996. Mathematical modelling of rods. Handbook of numerical analysis 4, 487–974.
Triantafyllidis, N., Scherzinger, W. M., Huang, H.-J., 2007. Post-bifurcation equilibria in the plane-strain test of a hyperelastic rectangular block. International Journal of Solids and Structures 44 (11–12), 3700–3719.
van der Hoeven, J., Grozin, A., Gubinelli, M., Lecerf, G., Poulain, F., Raux, D., 2013. GNU TEXmacs: a scientific editing platform. ACM Communications in Computer Algebra 47 (1–2), 59–61.
Wunderlich, W., 1962. Über ein abwickelbares Möbiusband. Monatshefte für Mathematik 66 (3), 276–289.
Xuan, C., Biggins, J., May 2017. Plateau-Rayleigh instability in solids is a simple phase separation. Physical Reivew E 95, 053106.